Convexification of high-dimension multi-label problems

Nicolas Papadakis, Jean-François Aujol, Vicent Caselles, Romain Yildizoglu

CONVEXIFICATION OF HIGH-DIMENSION MULTI-LABEL PROBLEMS

NICOLAS PAPADAKIS*, JEAN-FRANÇOIS AUJOL†, VICENT CASELLES‡, AND ROMAIN YILDIZOĞLU

Abstract. This paper is concerned with the problem of relaxing non convex functionals used in image processing into convex problems. We review most of the recently introduced convexification methods, and we propose a new one based on a probabilistic approach, which has the advantages of being intuitive and flexible. We investigate in detail the connections between the solution of the relaxed functional with a minimizer of the original one. As a case of study, we illustrate our theoretical analysis with numerical experiments, namely for the optical flow problem.

Key words. Multi-label problems, convex relaxation, segmentation, disparity and optical flow estimation

AMS subject classifications. 15A15, 15A09, 15A23

1. Introduction. This paper is concerned with image processing problems whose solutions are computed as the minimizer of some functional (see e.g. [4]). The considered functionals have a data term which depends on the considered application, and a regularization term. Many image processing problems can be modeled as the minimizers of non convex functionals. This non convexity may arise from the physics of the problem as in speckle noise removal [3]. It may be due to the non locality of the functional [5]. It can also come from the problem itself as in image segmentation [21, 13, 8, 19], optical flow computation [4, 23], ...

Non convexity of the functional to minimize may cause several issues. On the one hand, the solution of the problem may not exist, and even when it exists may be non unique. On the other hand, numerical algorithms to compute the solution may get stuck into local minima, and the numerical solution may depend heavily on the initialization choice (in the case of iterative algorithms).

For all these reasons, it is a major improvement when a non convex problem can be turned into a convex one. Some steps in this direction have been done in the last past years [9, 22, 2, 25, 23, 11, 27, 8, 17] within the mathematical image processing community. It has first been used for image segmentation as in [22], but it is now used for some higher dimensional problems such as optical flow [23]. The main idea of all these approaches is to introduce a new variable of higher dimension and solve a convex relaxed problem. If the original functional has some properties such as satisfying some layer cake formula, then a thresholding of the minimizer of the relaxed problem is a global minimizer of the original non convex problem (see [9, 22] for seminal works in this direction). Of course, due to the curse of dimension, resorting to higher dimensional variables increases the computation time. . This is the reason why convexification methods become more challenging when the dimension

* N. Papadakis is with the MOISE team (INRIA/CNRS), Laboratoire Jean Kuntzmann (LJK, UMR 5224), Campus de Saint Martin d'Hères, 38041 Grenoble, France. (e-mail: nicolas.papadakis@imag.fr)

†J-F. Aujol and R. Yıldızoğlu are with Univ. Bordeaux, Institut de Mathmatiques de Bordeaux (IMB, UMR 5251), 351 Cours de la Libration F-33400 Talence, France (e-mail: jaujol@math.u-bordeaux1.fr, ryildi@gmail.com)

‡V. Caselles is with the Departamento de Tecnologías de la Información y las Comunicaciones, Universitat Pompeu Fabra, Carrer de Roc Boronat 138, 08018 Barcelona, Spain. (e-mail: vicent.caselles@upf.edu)

of the variables is larger than one. This is the case for the optical flow problem (as compared with the segmentation one [22]), and this is the reason why we focus in this paper on the optical flow computation.

This paper is inspired by all the works recalled in the above paragraph. It proposes new convexification choices, based on a probabilistic modeling and leading to new algorithms. We illustrate our approach on the optical flow problem. Our numerical experiments validate the interest of the approach.

In all the proposed models, the regularization term is based on total variation. Such a term benefits from a layer cake formula thanks to the the coarea formula. This property plays a key role when one wants to relate the solution of the relaxed problem to the one of the original problem, as it will be detailed in the paper. Notice that some approaches such as [27] propose to use a truncated version of total variation, as it was shown to be useful in image restoration (see [4]). This non convexity of the regularization term may lead to better preservation of discontinuities. However, as explained in the next paragraph, an important aspect of our work lies in the study of how to get back from the solution of the relaxed problem to the one of the original problem. The natural setting for such a study is to consider a classical total variation term for the regularization and not a non convex version of it.

The main contributions of the paper are the following:

- We provide the reader with a review of most of the recently introduced convexification methods in image processing. We discuss in particular the connections between theses approaches, as well as some of their advantages and weaknesses.
- We introduce a new framework to relax image processing functionals into convex problems. Our approach is based on a probabilistic point of view which has the advantage of being flexible and intuitive.
- We discuss in details possible strategies to get back from a solution of the relaxed functionals to a minimizer of the original problem. As far as we know, this issue has not been investigated thoroughly in the literature yet. It is nevertheless a major problem, since computing a minimizer of the relaxed functional is of no interest if it is not related to a minimizer of the original problem.
- We illustrate the different approaches presented in the paper as well as the new ones on different applications including namely the optical flow problem. Since dimension is a major issue with convexification (as the dimension of the variables is increased when the functional is relaxed), we feel that optical flow is a good application to test the different frameworks (in view of the curse of dimension). Note that the different experiments focus on the ability of the proposed approach to recover global minima of the original problems.

The outline of the paper is as follows. We introduce the discrete framework we consider in Section 2. In particular, we detail the discretization choice, as well as the primal-dual algorithm that will be at the heart of all the numerical methods presented in the paper. For the sake of clarity, we first deal with the case of dimension 1 in Section 3. We recall the framework introduced in [25], and we then introduce a new one based on a probabilistic modeling. In all these approaches, the solution of the original problem is computed from the one of the relaxed problem with a simple thresholding strategy. We conclude Section 3 by showing the connection of our probabilistic framework with the approach of Chambolle et al in [11]. We then concentrate on the dimension 2 case in section 4. We first recall the approach of [23]

where the problem is relaxed independently for each variable (but which turns out to be polyconvex). We also present the approach of [27] which proposes a way to convexify the data term of the functional. However, the relationship with the original problem is not clear, and as we illustrate in the numerical section this approach does not lead to good solutions. We eventually recall the framework of [8] to get a general convexification. However, it seems to be unrealistic to be used in practice for the optical flow problem due to the use of Dijkstra algorithm to compute a complicated projection. Then we introduce our probabilistic framework in the 2D setting and we show the equivalence between the two last relaxed problems. However, contrary to the 1D setting, there is no simple thresholding strategy to get back from the solution of the relaxed problem to the solution of the original problem. This is the reason why we investigate in Section 5 the problem of computing a good solution of the original problem from the relaxed one. We then present extensive numerical examples for optical flow in Section 6.

2. Preliminaries.

2.1. General problem. We focus here on multi-label problems for image processing. Let Ω be the image domain: we assume Ω to be a non empty open bounded subset of $\mathbb{R}^2$ with Lipschitz boundary. We aim at estimating a set of N variables $u_i : \Omega \mapsto \Gamma_i$ (with $1 \leq i \leq N$) which take their values in a predefined discrete set containing M_i ordered elements: $\Gamma = \{u_0^i < \cdots < u_{M_i-1}^i\}$. This section is then dedicated to the minimization w.r.t $u = [u_1, \cdots, u_N]$ of the following class of functionals:

$$J_N(u) = \sum_{i=1}^{N} \int_\Omega |Du_i(x)| + \int_\Omega \rho(x, u(x))dx, \tag{2.1}$$

where ρ is a given positive data function and $\rho(x, u(x))$ represents the cost of assigning the values $u(x)$ to the pixel x. We only assume that ρ is a bounded function that can be non linear with respect to u. In the following, we will refer to the $1D$ case when $N = 1$.

The first terms $\int_\Omega |Du_i|$ contain the spatial regularization of the unknowns on the image domain. More precisely, they measure the integral of the perimeters of the level sets of u, assuming that u is a function of bounded variation (see [1] for more details). Such a term, introduced in image processing in the seminal work [26], is known as the total variation of u. This regularization is general and has been applied to a lot of image processing problems such as restoration [26], depth estimation [25], 3D reconstruction [18] or optical flow [29].

We now present some technical elements that will be used all along the paper.

2.2. Total variation.

Definition. For $u \in BV(\Omega, \mathbb{R})$ we have $\int_\Omega |Du| = \sup\{\int_\Omega u \mathrm{div} z, z \in C_c^1(\Omega), \| z \|_\infty \leq 1\}$ with $C_c^1(\Omega)$ the space of continuous functions with compact support on Ω (see [1]). Notice that in the case when u is a smooth function, then $\int_\Omega |Du| = \int_\Omega |\nabla u| \, dx$.

Discretization schemes. The discretization used for the spatial gradient operator D_x and its adjoint D_x^* are the classical ones. We consider the discrete regular grid $x = (\mathrm{x}, \mathrm{y})$, $1 \leq \mathrm{x} \leq L_\mathrm{x}$, $1 \leq \mathrm{y} \leq L_\mathrm{y}$ representing the domain Ω. Looking at the discrete gradient operator as a vector of matrices $D_x = [D_\mathrm{x}; D_\mathrm{y}]^T$, the chosen discretizations should satisfy (to have a discrete Gauss-Green formula without boundary terms): $\langle D_\mathrm{x} u, z_1 \rangle + \langle D_\mathrm{y} u, z_2 \rangle = \langle u, D_\mathrm{x}^* z_1 + D_\mathrm{y}^* z_2) \rangle$. To that end, one can consider finite

differences and take $D_x u(\mathrm{x},\mathrm{y})$ with a forward scheme and $D_{\mathrm{x}}^* z$ with a backward one. The gradient with respect to the first dimension then reads

$$D_{\mathrm{x}} u(\mathrm{x},\mathrm{y}) = \begin{cases} u(\mathrm{x}+1,\mathrm{y}) - u(\mathrm{x},\mathrm{y}) & \text{if } 1 \leq \mathrm{x} < L_{\mathrm{x}}, \\ 0 & \text{if } \mathrm{x} = L_{\mathrm{x}}. \end{cases}$$

The corresponding divergence operator is given by $D_x^* \mathbf{z} = D_{\mathrm{x}}^* z_1 + D_{\mathrm{y}}^* z_2$, where the gradient over the first dimension is taken as:

$$D_{\mathrm{x}}^* z(\mathrm{x},\mathrm{y}) = \begin{cases} z(\mathrm{x},\mathrm{y}) & \text{if } \mathrm{x} = 1, \\ z(\mathrm{x},\mathrm{y}) - z(\mathrm{x}-1,\mathrm{y}) & \text{if } 1 < \mathrm{x} < L_{\mathrm{x}}, \\ -z(\mathrm{x}-1,\mathrm{y}) & \text{if } \mathrm{x} = L_{\mathrm{x}}. \end{cases}$$

The discrete total variation of u can be defined as $\int_\Omega |D_x u| = \sum_{1 \leq \mathrm{x} \leq L_{\mathrm{x}}} |D_x u(\mathrm{x}, y)|$.

Let us denote by $\mathcal{B}$ the set of vector fields $\mathbf{z} = (z_1, z_2)$ with z_i defined on $\Omega \times \Gamma$ such that

$$\mathcal{B} = \{\mathbf{z},\ s.t.\ z_1^2(x,u_i) + z_2^2(x,u_i) \leq (u_i - u_{i-1})^2,\ \forall (x,u_i) \in \Omega \times \Gamma\}. \tag{2.2}$$

Then the total variation can be rewritten in its dual form $\int_\Omega |D_x u| = \max_{z \in \mathcal{B}} \langle u, D_x^* \mathbf{z} \rangle$.

2.3. Primal-dual algorithm.

Presentation. We recall the algorithm in [12]. U, Z are finite-dimensional vector spaces, we note $\langle ., . \rangle$ the standard inner products, $K : U \to Z$ is a linear operator and $G : U \to \mathbb{R} \cup \{\infty\}$ and $F^* : Z \to \mathbb{R} \cup \{\infty\}$ are convex functions. We want to solve

$$\min_{u \in U} \max_{z \in Z} \langle Ku, z \rangle + G(x) - F^*(y).$$

The algorithm

Algorithm 1 Primal-dual algorithm ([12])

$u^{k+1} = (I + \tau \partial G)^{-1}(u^k - \tau K^t z^k)$
$z^{k+1} = (I + \sigma \partial F^*)^{-1}(z^k - \sigma K(2u^{k+1} - u^k))$

with $(I + \tau\partial G)^{-1}(\hat{u}) := \arg\min_{u \in U} G(u) + \frac{1}{2\tau} \parallel u - \hat{u} \parallel^2$ and $\tau\sigma \parallel K \parallel^2 < 1$ converges to a saddle point in $O(\frac{1}{k})$. Notice that when K is the chosen discretized gradient operator, then $\|K\|^2 = 8$.

Proximal operator. If G is a convex proper lower semi continuous function, then $(I + \tau\partial G)^{-1}$ is the resolvent operator (which is a one to one mapping).

The proximity operator is defined by (see [20] for computation and details):

$$y = (I + \tau\partial G)^{-1}(x) = \mathrm{prox}_h^G(x) = \underset{u}{\mathrm{argmin}} \left\{ \frac{\|u - x\|^2}{2\tau} + G(u) \right\}. \tag{2.3}$$

We refer to [15] for examples of proximal operator computations. Notice that computing the proximal operator is itself a minimization problem. This computation amounts to a projection computation when G is the indicator of a closed convex set.

For instance, assume $G = \chi_{z\in\mathcal{B}}$, where $\mathcal{B}$ is the set of vector fields $\mathbf{z} = (z_1, z_2)$ defined by Equation (2.2). Then the resolvent operator $(I+\tau\partial G)^{-1}$ is (for any $\tau > 0$) the orthogonal projection:

$$P_{\mathcal{B}}(\mathbf{z}(x,u_i)) = \frac{(u_i - u_{i-1})\mathbf{z}(x,u_i)}{\max(u_i - u_{i-1}, ||\mathbf{z}(x,u_i)||)} \tag{2.4}$$

where $||\mathbf{z}(x,u_i)||^2 = z_1^2(x,u_i) + z_2^2(x,u_i)$.

Preconditionning. In the same framework as 2.3 we can precondition the algorithm in order to speed up the computation and to avoid the computation of $\| K \|$. We recall the algorithm of [24]:

Algorithm 2 Preconditioned primal-dual algorithm ([24])

$u^{k+1} = (I + T\partial G)^{-1}(u^k - TK^t z^k)$
$z^{k+1} = (I + \Sigma\partial F^*)^{-1}(z^k - \Sigma K(2u^{k+1} - u^k))$

with T and Σ symmetric positive definite matrices such that $\| \Sigma^{\frac{1}{2}} K T^{\frac{1}{2}} \|^2 < 1$ and $(I + T\partial G)^{-1}(\hat{u}) := \arg\min_{u\in U} G(u) + \frac{1}{2\tau}\left\langle T^{-1}(u-\hat{u}), u-\hat{u}\right\rangle$. It converges to a saddle point in $O(\frac{1}{k})$. We can take $T = \mathrm{diag}(\tau_1, ..., \tau_n)$ and $\Sigma = \mathrm{diag}(\sigma_1, ..., \sigma_m)$ with $\tau_j < \frac{1}{\sum_{i=1}^m |K_{i,j}|}$, $\sigma_i < \frac{1}{\sum_{j=1}^n |K_{i,j}|}$.

3. Convexification of the $1D$ multi-label problem. This section is dedicated to the $1D$ case, where we only want to estimate 1 unknown for each pixel of an image and minimize the functional:

$$J_1(u) = \int_\Omega |Du(x)| + \int_\Omega \rho(x, u(x))dx. \tag{3.1}$$

With u taking its values in $\Gamma = \{u_0 < \cdots < u_{M-1}\}$.

For the segmentation of a grayscale image $I : x \in \Omega \mapsto I(x) \in [0,1]$ in M gray color labels $\Gamma = \{0, 1/(M-1), \cdots 1\}$, the function would read: $\rho(x,u(x)) = (I(x) - u(x))^2$. In the case of disparity estimation between two images I_1 and I_2, with disparity values in $\Gamma = \{0, 1, \cdots, M-1\}$, the cost would be: $\rho(x,u(x)) = (I_1(x) - I_2(x + u(x))^2$.

3.1. Convexification of the $1D$ multi-label problem with upper level sets. We briefly recall here the convexification technique of Pock et al. [25]. The idea is to write the non-linearities of the functional $J_1(u)$ in a convex way, by introducing an auxiliary variable $\phi : \Omega \times \Gamma \mapsto \{0,1\}$ that represents the different values of u. The treatment here will be heuristic. Let

$$\phi(x,s) = H(u(x) - s), \tag{3.2}$$

where H is the Heaviside function ($H(r) = 1$ if $r \geq 0$, and 0 otherwise).

The unknown u can then be recovered from ϕ by the layer cake formula as

$$u(x) = u_0 + \sum_{i=1}^{M-1} (u_i - u_{i-1})\phi(x, u_i). \tag{3.3}$$

Using the coarea formula, we find

$$\begin{aligned}
\int_\Omega |Du(x)| &= \int_s \int_\Omega |D\mathbf{1}_{u\geq s}(x)|dxds = \sum_{i=1}^{M-1}(u_i - u_{i-1})\int_\Omega |D\mathbf{1}_{u\geq u_i}(x)|dx \\
&= \sum_{i=1}^{M-1}(u_i - u_{i-1})\int_\Omega |D_x\phi(x,u_i)|dx \\
\int_\Omega \rho(x,u(x)) &= \int_\Omega \sum_{i=0}^{M-1}\rho(x,u_i)\mathbf{1}_{u=u_i}(x)dx \\
&= \sum_{i=1}^{M-2}\int_\Omega \rho(x,u_i)(\phi(x,u_i)-\phi(x,u_{i+1}))dx + \int_\Omega \rho(x,u_{M-1})dx.
\end{aligned} \tag{3.4}$$

Hence we can rewrite functional (3.1) as a function of ϕ instead of u.

$$\begin{aligned}
J_1(u) =& \sum_{i=1}^{M-1}(u_i - u_{i-1})\int_\Omega |D_x\phi(x,u_i)|dx + \sum_{i=1}^{M-2}\int_\Omega \rho(x,u_i)(\phi(x,u_i)-\phi(x,u_{i+1}))dx \\
&+ \int_\Omega \rho(x,u_{M-1})dx \\
=& J(\phi),
\end{aligned} \tag{3.5}$$

and we are thus led to consider the minimizing problem:

$$\min_{\phi\in\bar{\mathcal{A}}_1} J(\phi), \tag{3.6}$$

where

$$\bar{\mathcal{A}}_1 = \{\phi \in BV(\Omega\times\Gamma,\{0;1\}) \text{ such that } \ \phi(x,u_0)=1,\ \phi(x,u_i)\geq\phi(x,u_{i+1})\}. \tag{3.7}$$

Following [25], we have the following theorem.

THEOREM 3.1. *The layer cake formula (3.3) defines a bijection f between $\mathcal{A}_0$ and $BV(\Omega,\{0,1\})$ such that $J_1(f(\phi)) = J(\phi)$ (3.1).*

Proof. We only need to verify that f is a bijection, the functional equality being given by (3.5). Let $\phi\in\mathcal{A}_0$, $x\in\Omega$, there exists j such that $\phi(x,u_i)=1$ for $i\leq j$ and $\phi(x,u_i)=0$ for $i>j$, so $f(\phi)(x) = u_0 + \sum_{i=1}^{M-1}(u_i-u_{i-1})\phi(x,u_i) = u_j\in\Gamma$. $f(\phi)$ is of bounded variations by (3.5), so f is a bijection. ∎

Functional (3.5) is convex in ϕ. To find the global minimum of (3.1), one can find a ϕ minimizing (3.5), and then recover u from ϕ. Care must be taken to ensure that it is possible to compute u from ϕ. In particular, ϕ must be binary and decreasing with s. Unfortunately, the set of such functions ϕ is not convex.

To recover convexity, the function ϕ should be allowed to take values on $[0,1]$. We introduce a convex set of admissible functions

$$\mathcal{A}_1 = \{\phi \in BV(\Omega\times\Gamma,[0,1]) \text{ such that } \phi(x,a)=1,\ \phi(x,u_i)\geq\phi(x,u_{i+1})\}, \tag{3.8}$$

and the convex problem

$$\min_{\phi\in\mathcal{A}_1} J(\phi). \tag{3.9}$$

Following [25], we have the following theorem.

THEOREM 3.2. *Let ϕ^* be a solution of (3.9), then for almost any threshold μ, $H(\phi^* - \mu)$ is a solution of (3.9) and of (3.6).*

Proof. Let us consider the solution ϕ^* of the relaxed problem (3.9). By the coarea formula we obtain:

$$\int_\Omega |D\phi^*| = \int_0^1 \left(\int_\Omega |DH(\phi^* - \mu)| \right) d\mu. \tag{3.10}$$

Furthermore

$$\begin{aligned} \int_\Omega \rho(x,u_i)\phi^*(x,u_i) &= \int_\Omega \rho(x,u_i) \int_0^1 H(\phi^*(x,u_i) - \mu) d\mu \\ &= \int_0^1 d\mu \int_\Omega \rho(x,u_i) H(\phi^*(x,u_i) - \mu). \end{aligned} \tag{3.11}$$

Using (3.5) we have that $J(\phi^*) = \int_{\mu=0}^1 J(H(\phi^* - \mu))d\mu$.

Let us now assume that $B := \{\mu \in [0,1],\ H(\phi^* - \mu)$ is not a global solution of the non convex problem (3.6)$\}$ has a strictly positive measure. Then there exists $\phi' \in \mathcal{A}_1$ such that $J(\phi') < J(H(\phi^* - \mu))$ for every μ in B. This implies that $J(\phi') = \int_0^1 J(\phi')d\mu < \int_0^1 J(H(\phi^* - \mu))d\mu = J(\phi^*)$ which is impossible by definition of ϕ^*. ∎

Therefore, a global minimum of (3.1) can be recovered as a "cut" of ϕ. For almost any threshold $\mu \in [0,1]$, defining $\phi_\mu = \mathbf{1}_{\phi^* \geq \mu}$,

$$u(x) = u_0 + \sum_{i=1}^{M-1} \phi_\mu(x,u_i). \tag{3.12}$$

is a global minimum of (3.1).

3.1.1. Numerical optimization. The previous minimization problem (3.9) can be written as a primal-dual problem:

$$\min_{\phi\in\mathcal{A}_1} \max_{\mathbf{z}\in\mathcal{B}, z_3\in\mathcal{C}} \int_\Omega \sum_{i=1}^{M-1} (u_i - u_{i-1}) D_x\phi(x,u_i)\cdot\mathbf{z}(x,u_i)dx + \int_\Omega \sum_{i=0}^{M-1} D_u\phi(x,u_i) z_3(x,u_i)dx, \tag{3.13}$$

where the operator D_u and its adjoint D_u^* are defined as:

$$D_u\phi(x,u_i) = \begin{cases} \phi(x,u_{i+1}) - \phi(x,u_i) & \text{if } i < M-1, \\ 0 & \text{otherwise,} \end{cases} \tag{3.14}$$

$$D_u^* z(x,u_i) = \begin{cases} z(x,u_i) & \text{if } i = 0, \\ z(x,u_i) - z(x,u_{i-1}) & \text{if } 0 < i < M-1, \\ -z(x,u_{i-1}) & \text{if } i = M-1. \end{cases} \tag{3.15}$$

The orthogonal projection onto $\mathcal{B}$ denoted by $P_{\mathcal{B}}$ is recalled in Equation (2.4). The last dual variable $z_3 \in \Omega \times \Gamma$ is finally defined on the set:

$$\mathcal{C} = \{z_3, \text{ s.t. } |z_3(x,u_i)| \leq \rho(x,u_i), \forall (x,u_i) \in \Omega \times \Gamma\} \tag{3.16}$$

with the projection operator:

$$P_{\mathcal{C}}(z_3(x,u_i)) = \begin{cases} \frac{z_3(x,u_i)}{|z_3(x,u_i)|}\rho(x,u_i) & \text{if } |z_3(x,u_i)| > \rho(x,u_i) \\ z_3(x,u_i) & \text{otherwise.} \end{cases}$$

We end up with the algorithm 3 to minimize the energy (3.5)

Algorithm 3 Minimizing the 1D energy (3.5)

Initialize $\phi^0(.,u_i) = \bar{\phi}^0(.,u_i) = \frac{u_{M-1}-u_i}{u_{M-1}-u_0}$, $z_i = 0$, chose $\theta \in [0,1]$ and $\sigma, \tau > 0$ such that $\sigma\tau < \frac{1}{8}$
while $||\phi^k - \phi^{k-1}|| > \epsilon$ **do**
$\mathbf{z}^{k+1} = P_{\mathcal{B}}\left(\mathbf{z}^k + \sigma D_x \bar{\phi}^k\right)$
$z_3^{k+1} = P_{\mathcal{C}}\left(z_3^k + \sigma D_u \bar{\phi}^k\right)$
$\phi^{k+1} = P_{\mathcal{A}_1}\left(\phi^k - \tau\left(D_x^* \mathbf{z}^{k+1} + D_u^* z_3^{k+1}\right)\right)$,
$\bar{\phi}^{k+1} = \phi^{k+1} + \theta(\phi^{k+1} - \phi^k)$
end while

3.1.2. Important detail. The convex set $\mathcal{A}_1$ defined in Equation (3.8) involves the negativity of the quantities $\phi(x,u_{i+1}) - \phi(x,u_i)$. In the original paper [25], such property has not been considered and the projection was just:

$$P_{\mathcal{A}_1}(\phi(x,u_i)) = \begin{cases} 1 & \text{if } i = 0, \\ \max(0, \min(1, \phi(x,u_i))) & \text{if } 0 < i < M-1, \\ 0 & \text{if } i = M-1. \end{cases} \tag{3.17}$$

This issue has been fixed in [10], where an iterative algorithm inspired from the Dijkstra algorithm is introduced to define $P_{\mathcal{A}_1}$ and impose the constraint pointwise, for each $x \in \Omega$.

This is the main drawback of this convexification, as the process involves time consuming iterative projections (and the primal projection $P_{\mathcal{A}_1}$ is in theory only exact with an infinite number of Dijkstra iterations). We now explain how a slight modification of the previous approach leads to simple projections for any $N \geq 1$. We found out that the proposed approach is connected with the recent one of [11], while we here propose an exact and simple dual projection.

3.2. A new convexification based on a probabilistic point of view. Let us recall that the functional to minimize in order to obtain a label assignation map u reads:

$$J_1(u) = \int_\Omega |Du(x)| + \int_\Omega \rho(x,u(x))dx. \tag{3.18}$$

The idea is to model the possible values of the data function ρ with

$$\min_{u\in\Gamma}\int_\Omega \rho(x,u(x))dx = \min_{w\in\mathcal{D}_1}\int_\Omega \sum_{i=0}^{M-1}\rho(x,u_i)w(x,u_i)dx,$$

where $w(x,u_i)$ represents the probability of assigning the label u_i to the pixel x. The equivalence with the original problem is obtained by considering a particular space for w that corresponds to a single assignation for each pixel $x\in\Omega$: there exists a unique $\tilde{s}\in\Gamma$ with $w(x,\tilde{s})=1$ and $w(x,s)=0$ for $s\neq\tilde{s}$. Since probabilities with binary values are involved, this problem of assignation is not convex.

The new variable w is then relaxed within the convex space

$$\mathcal{D}_1 = \left\{ w:\Omega\times\Gamma\mapsto[0,1],\ \text{s.t.}\ \sum_i w(x,u_i)=1,\ \forall x\in\Omega \right\}. \tag{3.19}$$

The Total Variation of u can be rewritten in terms of w as:

$$\begin{aligned}\int_\Omega |Du| &= \int_\Omega \sum_{i=1}^{M-1}(u_i-u_{i-1})|D_x H(u(x)-u_i)|ds \\ &= \int_\Omega \sum_{i=1}^{M-1}(u_i-u_{i-1})\left|D_x\left(\sum_{j\geq i}w(x,u_j)\right)\right|dx,\end{aligned}$$

and the functional finally is:

$$J_w(w) = \int_\Omega \sum_{i=1}^{M-1}(u_i-u_{i-1})\left|D_x\left(\sum_{j\geq i}w(x,u_j)\right)\right|dx + \int_\Omega\sum_{i=0}^{M-1}\rho(x,u_i)w(x,u_i)dx. \tag{3.20}$$

The problem of minimizing (3.20) w.r.t $w\in\mathcal{D}_1$ is convex and a global minimum can be estimated with the previously introduced optimization method involving a dual formulation of the TV term.

3.2.1. Numerical optimization. The dual formulation consists in rewriting the regularization term as:

$$\begin{aligned}&\int_\Omega \sum_{i=1}^{M-1}(u_i-u_{i-1})\left|D_x\left(\sum_{j\geq i}w(x,u_j)\right)\right|dx \\ =&\max_{\mathbf{z}\in\mathcal{B}}\int_\Omega\sum_{i=1}^{M-1}\left(\sum_{j\geq i}w(x,u_j)\right)D_x^*\mathbf{z}(x,u_i)dx,\end{aligned}$$

where the variable $\mathbf{z}=(z_1,z_2)$, with $z_k\in\Omega\times\Gamma$, is defined on the convex set given by Equation (2.2) that we recall here:

$$\mathcal{B}=\{\mathbf{z},\ s.t.\ z_1^2(x,u_i)+z_2^2(x,u_i)\leq(u_i-u_{i-1})^2,\ \forall(x,u_i)\in\Omega\times\Gamma\}, \tag{3.21}$$

with the convention that $\mathbf{z}(.,u_0)=0$ since the level u_0 is useless for the TV energy of w as $\sum_{j\geq 0} w(x,u_j)=1$, $\forall x\in\Omega$.

The projection operator $P_{\mathcal{B}}$ is given in Equation (2.4).

The projection of w onto the convex set $\mathcal{D}_1$ (defined in Equation (3.19)) can finally be done point-wise for each pixel x with the projection of $w(x,.)$ onto a simplex of dimension M through the operator $P_{\mathcal{D}_1}:\mathbb{R}^{|\Omega|M}\rightarrow\mathcal{D}_1$ (see [14] for a fast implementation).

A sketch of the process for estimating w^* following the Primal-Dual approach of [12] and the discretizations given in section 2 is given in Algorithm 4.

Algorithm 4 Minimizing the 1D energy (3.20)

Initialize $w^0=\bar{w}^0=\frac{1}{M}$, $\mathbf{z}^0=0$, chose $\theta\in[0,1]$ and $\sigma,\tau>0$ such that $\sigma\tau<\frac{1}{8M^2}$
while $||w^k-w^{k-1}||>\epsilon$ **do**
$\mathbf{z}^{k+1}(.,u_i)=P_{\mathcal{B}}\left(\mathbf{z}^k(.,u_i)+\sigma D_x\left(\sum_{l\geq i}\bar{w}^k(.,u_l)\right)\right),\qquad \forall u_i\in\Gamma$
$\tilde{w}(.,u_i)=w^k(.,u_i)-\tau\left(\rho(.,u_i)+\sum_{l\leq i}D_x^*\mathbf{z}^{k+1}(.,u_l)\right),\qquad \forall u_i\in\Gamma$
$w^{k+1}=P_{\mathcal{D}_1}(\tilde{w})$,
$\bar{w}^{k+1}=w^{k+1}+\theta(w^{k+1}-\bar{w}^k)$
end while

With respect to the previous section and the estimation of $\phi\in\mathcal{A}_1$ (defined in Equation (3.8)), the computational complexity is increased with the term $\sum_{l\geq i}w(x,u_l)$. However, the projection of the variable w is here exact [14], and not iterative as in the previous formulation. This makes the computational time of one iteration k of both approaches equivalent, when considering two iterations of the Dijkstra algorithm to project ϕ on $\mathcal{A}_1$ (whereas 2 Dijkstra iterations are not sufficent in may cases). It is also relevant to note that preconditionning techniques can be considered to speed-up the current process [24], as illustrated in Algorithm 5.

Algorithm 5 Minimizing the 1D energy with the preconditioned algorithm (3.20)

Initialize $w^0=\bar{w}^0=\frac{1}{M}$, $\mathbf{z}^0=0$, take $\sigma_i=\frac{1}{2i}$, $\tau_i=\frac{1}{4(M+1-i)}$.
while $||w^k-w^{k-1}||>\epsilon$ **do**
$w^{k+1}=P_{\mathcal{D}_1}\left(\left(w^k(.,u_i)-\tau_i\left(\rho(.,u_i)+\sum_{l\leq i}D_x^*\mathbf{z}^{k+1}(.,u_l)\right)\right)_i\right)$,
$\mathbf{z}^{k+1}(.,u_i)=P_{\mathcal{B}}\left(\mathbf{z}^k(.,u_i)+\sigma_i D_x\left(\sum_{l\geq i}(2w^{k+1}-w^k)(.,u_l)\right)\right),\qquad \forall u_i\in\Gamma$
end while

3.2.2. Equivalence with the original problem (3.18). We now have to show that a solution of the original problem (i.e. a label assignation) can be obtained from the computed solution w^*.

First of all, let us observe the relation with the previous section 3, where the convexification is done with $\phi=H(u(x)-s)$, and the functional to minimize for $\phi\in\mathcal{A}_1$ is:

$$J(\phi)=\sum_{i=1}^{M-1}(u_i-u_{i-1})\int_\Omega|D_x\phi(x,u_i)|dx+\sum_{i=1}^{M-1}\int_\Omega\rho(x,u_i)(\phi(x,u_i)-\phi(x,u_{i+1}))dx \tag{3.22}$$

with

$$\mathcal{A}_1 = \{\phi \in BV(\Omega \times \Gamma, [0,1]) \text{ such that } \phi(x,u_O) = 1,\ \phi(x,u_i) \geq \phi(x,u_{i+1})\}. \quad (3.23)$$

PROPOSITION 3.3. *There exists a bijection f between the convex sets $\mathcal{A}_1$ and $\mathcal{D}_1$, with $f(\phi)(x,u_i) = \phi(x,u_i) - \phi(x,u_{i+1})$ and $f^{-1}(w)(x,u_i) = \sum_{j\geq i} w(x,u_j)$.*

Hence, setting $\phi(x,u_i) = \sum_{j\geq i} w(x,u_j)$ and observing that $w(x,u_i) = \phi(x,u_i) - \phi(x,u_{i+1})$, we can now see that

$$\begin{aligned} \min_{\phi\in\mathcal{A}_1} J(\phi) &= \min_{w\in\mathcal{D}_1} J(f^{-1}(w)) \\ &= \min_{w\in\mathcal{D}_1} J_w(w). \end{aligned} \quad (3.24)$$

As a consequence, if w^* is a global minimizer of the energy (3.20), then $\phi^* = f^{-1}(w^*)$ is a global minimizer of the energy (3.22).

We know from section 3 that the problem in ϕ is convex and that for almost any threshold μ then $H(\phi^* - \mu)$ is also a global solution. We can therefore build ϕ^* from w^* and threshold to recover a global solution of the original problem.

3.3. Connections with the approach of Chambolle et al [11]. Notice that in [11], the authors have tackled the related problem of minimal partitions. Each label i corresponds to a couple $(s,t)_i$ and a cost σ_{ij} is given to represent distance between labels i and j. In our problem $\sigma_{ij} = |s_i - s_j|$. The problem is then to minimize w.r.t to a label map $\lambda : x \in \Omega \mapsto \lambda(x) = i \in [1;N]$, the energy:

$$J(\lambda) = \int_\Omega \rho(x,\lambda(x)) + \sum_i \sum_j \sigma_{ij} |\partial\Omega_i \cap \partial\Omega_j|,$$

where the partition of Ω in N areas is defined as:

$$\Omega_i = \{x \in \Omega \, s.t. \, \lambda(x) = i\}.$$

The problem is relaxed by minimizing

$$\min_{w\in\mathcal{D}_1} \Psi(Dw) + \int_\Omega \rho(x,u_i) w(x,u_i) dx \quad (3.25)$$

with $\Psi(Dw) := \sup_{(q)\in K} \int_\Omega q_{ij}.D_x w(x,u_i,)$, $K = \{(q_i), |q_i - q_j| \leq |u_i - u_j|\}$. This is equivalent to our formulation. Indeed, we have

$$\begin{aligned} \sum_{i=1}^{M-1} (u_i - u_{i-1}) \int_\Omega |D \sum_{j\geq i} w_j| &= \sup_{|q_i|\leq u_i - u_{i-1}} \sum_{i=1}^{M-1} \int_\Omega q_i D \sum_{j\geq i} w_j \\ &= \sup_{|q_j|\leq u_i - u_{i-1}} \int_\Omega \sum_{j=1}^{N} Dw_j \left(\sum_{i\leq j} q_i \right). \end{aligned} \quad (3.26)$$

Setting $q'_j = \sum_{i \leq j} q_i$, we have $q_j = q'_{j+1} - q'_j$ and :

$$\sum_{i=1}^{M-1} (u_i - u_{i-1}) \int_\Omega |D \sum_{j \geq i} w_j| = \sup_{|q'_{j+1} - q'_j| \leq u_i - u_{i-1}} \sum_{j=1}^{M-1} \int_\Omega q'_j Dw_j, \tag{3.27}$$

which gives exactly the set $K = \{|q'_{j+1} - q'_j| \leq u_i - u_{i-1}\}$ they prove to be the best relaxation for the minimal partition problem. Our approach is similar to [11], but with a different point of view (a probabilistic one).

4. Convexification of the $2D$ multi-label problem. We now look at the following class of functionals:

$$J_2(u, v) = \int_\Omega |Du(x)| + \int_\Omega |Dv(x)| + \int_\Omega \rho(x, u(x), v(x))dx, \tag{4.1}$$

defined for the variables $u(x)$ and $v(x)$ taking their values in the discrete sets $\Gamma^u = \{u_0 < \cdots u_{M-1}\}$ and $\Gamma^v = \{v_0 < \cdots v_{M-1}\}$. For sake of clarity we will now consider that the discretization step of Γ^u and Γ^v is uniform, so that $u_i - u_{i-1} = \Delta_u$, and $v_i - v_{i-1} = \Delta_v$ for $i = 1 \cdots M - 1$.

Let us give an example of the data term ρ for the problem of the optical flow estimation between two images. In this case, we seek the $2D$ vector field corresponding to the flow $w(x) = (u(x), v(x))$ going from image I_1 to image I_2.

The field $w(x) = (u(x), v(x))$ then represents the displacement field of pixels x of image I_1. The cost function ρ can then be defined as:

$$\rho(x, u(x), v(x)) = |I_1(x) - I_2(x + w(x))|. \tag{4.2}$$

4.1. Independent convexification. In this part, we consider the natural extension of the previous section that consists in introducing an auxiliary function for each variable to estimate. Following the probability formulation of section 3.2, we now have two functions w_u and w_v that belongs to the convex set of admissible functions $\mathcal{D}_1$, defined in (3.19). The regularization terms of energy (4.1) can therefore be written as

$$\begin{aligned} \int_\Omega |Du| &= \int_\Omega \sum_{i=1}^{M-1} (u_i - u_{i-1}) |D_x H(u(x) - u_i)| ds \\ &= \Delta_u \int_\Omega \sum_{i=1}^{M-1} \left| D_x \left(\sum_{j \geq i} w_u(x, u_j) \right) \right| dx \\ \int_\Omega |Dv| &= \Delta_v \int_\Omega \sum_{i=1}^{M-1} \left| D_x \left(\sum_{j \geq i} w_v(x, v_j) \right) \right| dx \end{aligned} \tag{4.3}$$

Let us now detail how to treat the data term.

4.1.1. Non convex data term. Using the previously introduced notations, the data term reads

$$\begin{aligned}\int_\Omega \rho(x,u(x),v(x))dx &= \int_\Omega \sum_{i=0}^{M-1}\sum_{j=0}^{M-1} \rho(x,u_i,v_j)\mathbf{1}_{u=u_i}(x)\mathbf{1}_{v=v_j}(x)dx \\ &= \int_\Omega \sum_{i=0}^{M-2}\sum_{j=0}^{M-2} \rho(x,u_i,v_j)\left((H(u(x)-u_i)) - H(u(x)-u_{i+1})\right) \\ &\quad \left(H(v(x)-v_j) - H(v(x)-v_{j+1})\right)\big)\,dx \\ &= \sum_{i=0}^{M-1}\sum_{j=0}^{M-1}\int_\Omega \rho(x,u_i,v_j)w_u(x,u_i)w_v(x,v_j),\end{aligned} \tag{4.4}$$

and we end up with the following problem

$$\min_{(w_u,w_v)\in\mathcal{D}_1\times\mathcal{D}_1} J(w_u,w_v), \tag{4.5}$$

with

$$\begin{aligned}J(w_u,w_v) = &\sum_{i=0}^{M-1}\sum_{j=0}^{M-1}\int_\Omega \rho(x,u_i,v_j)w_u(x,u_i)w_v(x,v_j) \\ &+ \Delta_u\int_\Omega \sum_{i=1}^{M-1}\left|D_x\left(\sum_{j\geq i} w_u(x,u_j)\right)\right|dx + \Delta_v\int_\Omega\sum_{i=1}^{M-1}\left|D_x\left(\sum_{j\geq i} w_v(x,v_j)\right)\right|dx.\end{aligned} \tag{4.6}$$

The data term of this energy is not convex in variables w_u and w_v, so that alternate minimization over w_u and w_v will only able to reach a local minima of the problem (4.5). Such local minima can be obtained in the following way. Assuming that w_v (resp. w_u) is known, the energy is minimized with respect to w_u (resp. w_v) until convergence. In both cases, we can linearize with respect to the optimized variable and recover the original $1D$ problem. For instance, when optimizing with respect to ϕ, we have the problem

$$\min_{w_u}\Delta_u\int_\Omega\sum_{i=1}^{M-1}\left|D_x\left(\sum_{j\geq i}w_u(x,u_j)\right)\right|dx + \sum_{i=0}^{M-1}\int_\Omega \rho_u(x,u_i)w_u(x,u_i) \tag{4.7}$$

where the data value ρ_u is obtain by integration over the dimension associted to v:

$$\rho_u(x,u_i) = \sum_{j=0}^{M-1}\rho(x,u_i,v_j)w_v(x,v_j) \tag{4.8}$$

and the numerical optimization method of section 3.1.1 can be used to minimize (4.7). At convergence of the process, the obtained local minima (w_u^*, w_v^*) can be used to build $\phi_u = f(w_u^*)$ and $\phi_v = f(w_v^*)$, with the function f defined in Proposition 3.3.

By thresholding such functions, we can produce an admissible function of the original non convex problem : $u^*(x) = u_0 + \Delta_u\sum_{i=1}^{M-1}\phi_u(x,u_i,)$ and $v^*(x) = v_0 + \Delta_v\sum_{i=1}^{M-1}\phi_v(x,v_i)$. However, we here have no information on the obtained couple $(u^*(x),v^*(x))$, which has no reason to be a local extremum.

Algorithm 6 Minimizing the 2D non-convex energy (4.6)

Initialize $w_u^0 = \bar{w}_u^0 = \frac{1}{M}$, $w_v^0 = \bar{w}_v^0 = \frac{1}{M}$,$\mathbf{z}_u^0 = \mathbf{z}_v^0 = 0$, chose $\theta \in [0,1]$ and $\sigma, \tau > 0$ such that $\sigma\tau < \frac{1}{8M}$

while $||w_u^k - w_u^{k-1}|| + ||w_v^k - w_v^{k-1}|| > \epsilon$ **do**

Compute $\rho_u(x,u_i) = \sum_{j=0}^{M-1} \rho(x,u_i,v_j) w_v^k(x,v_j)$

while $||w_u^k - w_u^{k-1}|| > \epsilon$ **do**

$$\mathbf{z}_u^{k+1}(.,u_i) = P_{\mathcal{B}}\left(\mathbf{z}_u^k(.,u_i) + \sigma D_x\left(\sum_{l\geq i} \bar{w}_u^k(.,u_l)\right)\right), \qquad \forall u_i \in \Gamma^u$$

$$\tilde{w}_u(.,u_i) = w_u^k(.,u_i) - \tau\left(\rho_u(.,u_i) + \sum_{l\leq i} D_x^* \mathbf{z}_u^{k+1}(.,u_l)\right), \qquad \forall u_i \in \Gamma^u$$

$$w_u^{k+1} = P_{\mathcal{D}_1}(\tilde{w}_u),$$

$$\bar{w}_u^{k+1} = w_u^{k+1} + \theta(w_u^{k+1} - \bar{w}_u^k)$$

end while

Compute $\rho_v(x,v_j) = \sum_{i=0}^{M-1} \rho(x,u_i,v_j) w_u^{k+1}(x,u_i)$

while $||w_v^k - w_v^{k-1}|| > \epsilon$ **do**

$$\mathbf{z}_v^{k+1}(.,v_j) = P_{\mathcal{B}}\left(\mathbf{z}_v^k(.,v_j) + \sigma D_x\left(\sum_{l\geq j} \bar{w}_v^k(.,v_l)\right)\right), \qquad \forall v_j \in \Gamma^v$$

$$\tilde{w}_v(.,v_j) = w_v^k(.,v_j) - \tau\left(\rho_v(.,v_j) + \sum_{l\leq j} D_x^* \mathbf{z}_v^{k+1}(.,v_l)\right), \qquad \forall v_i \in \Gamma^v$$

$$w_v^{k+1} = P_{\mathcal{D}_1}(\tilde{w}_v),$$

$$\bar{w}_v^{k+1} = w_v^{k+1} + \theta(w_v^{k+1} - \bar{w}_v^k)$$

end while

end while

Remark. When looking at the continuous formulation (Δ_u and Δ_v tending to 0) within the upper level sets framework, this corresponds to introduce 2 auxiliary variables ϕ_u and ϕ_v defined in $\mathcal{A}_1$, and the data term reads:

$$\int_{\Gamma^u}\int_{\Gamma^v}\int_{\Omega} \rho(x,s,t)\partial_s\phi_u(x,s)\partial_t\phi_v(x,t)dsdtdx.$$

It has been noticed in [23] that this term is polyconvex in the sense of [7] as it involves the determinant of the Jacobian Matrix in (s,t):

$$\begin{pmatrix} \partial_s\phi & \partial_t\phi \\ \partial_s\psi & \partial_t\psi \end{pmatrix} = \begin{pmatrix} \partial_s\phi & 0 \\ 0 & \partial_t\psi \end{pmatrix}.$$

Polyconvex functionals are quasiconvex. As quasiconvexity is the right extension of the notion of convexity for vector valued functions, it guarantees, under assumptions, the existence of minimizers and the well-posedness (in a certain sense) of the energies. Since the probability formulation shares the properties of the upper level sets one, it may explain the good behavior of the non convex approach on real experiments that will be detailed in the application section.

4.1.2. Convexification of the data term. To tackle properly the whole energy, some convex relaxations of the data term have been proposed in [16, 27]. The idea of [27] is to compute the biconjugate of the data term with the Legendre-Fenchel transform in order to obtain a tight relaxation. This leads to reformulate the data

term as:

$$\begin{aligned}&\sum_{i=0}^{M-1}\sum_{j=0}^{M-1}\int_\Omega \rho(x,u_i,v_j)w_u(x,u_i)w_v(x,v_j)\\ =&\max_{(q_u,q_v)\in\mathcal{Q}}\sum_{i=0}^{M-1}\int_\Omega \left(w_u(x,u_i)q_u(x,u_i)+w_v(x,v_i)q_v(x,v_i)\right),\end{aligned}$$

where two other auxiliary variables $q_u(x,u_i)$ and $q_v(x,v_j)$ have been introduced. They are defined in the convex set:

$$\begin{aligned}\mathcal{Q}=&\{q_u:\Omega\times\Gamma_u\mapsto\mathbb{R},\ q_v:\Omega\times\Gamma_v\mapsto\mathbb{R},\\ &\text{s.t. } q_u(x,u_i)+q_v(x,v_j)\leq\rho(x,u_i,v_j)\,\forall x\in\Omega,\ 0\leq i,j\leq M-1\}.\end{aligned}$$

We end up with the following energy to minimize w.r.t w_u andw_v:

$$\begin{aligned}J(w_u,w_v)=&\max_{(q_u,q_v)\in\mathcal{Q}}\sum_{i=0}^{M-1}\int_\Omega \left(w_u(x,u_i)q_u(x,u_i)+w_v(x,v_i)q_v(x,v_i)\right)\\ &+\Delta_u\int_\Omega\sum_{i=1}^{M-1}\left|D_x\left(\sum_{j\geq i}w_u(x,u_j)\right)\right|dx+\Delta_v\int_\Omega\sum_{i=1}^{M-1}\left|D_x\left(\sum_{j\geq i}w_v(x,v_j)\right)\right|dx.\end{aligned}\tag{4.9}$$

As the orthogonal projection on $\mathcal{Q}$ can not be written explicitely, we can not define the corresponding proximal operator needed by the primal-dual algorithm of [12] can not be formulated directly for the new variables (q_u,q_v). One solution could be to do inner loops in order to approximate the proximal operator related to the projection on $\mathcal{Q}$. Nevertheless, the authors of [27] chose to consider a Lagrange multiplier to enforce the constraint $q_u(x,u_i)+q_v(x,v_j)\leq\rho(x,u_i,v_j)$. Their process then consists in maximizing over (q_u,q_v) with an Uzawa's algorithm parameterized with an appropriate time step τ. Such approach for the management of the constraint leads to introduce another variable and appeared to be quite sensible numerically in our experiments.

As a consequence, we here propose an explicit projection into the convex set $\mathcal{Q}$ in order to prevent the observed numerical instabilities. This projection, denoted as $P_\mathcal{Q}$, is not orthogonal, but projects into $\mathcal{Q}$ by computing for each pixel $x\in\Omega$ the residual: $r(x,u_i,v_j)=\rho(x,u_i,v_j)-(q_u(x,u_i)+q_v(x,v_j))$ and defines:

$$\begin{aligned}\Big[P_\mathcal{Q}(q_u(x,u_i)),&P_\mathcal{Q}(q_v(x,v_j))\Big]\triangleq P_\mathcal{Q}\left(\Big[q_u(x,u_i),q_v(x,v_j)\Big]\right)\\ &=[q_u(x,u_i)-\max_{v_j}r(x,u_i,v_j),q_v(x,v_j)-\max_{u_i}r(x,u_i,v_j)]\end{aligned}$$

which ensures that $P_\mathcal{Q}(q_u(x,u_i))+P_\mathcal{Q}(q_v(x,v_j))\leq\rho(x,u_i,v_j)$, $\forall x\in\Omega$ and $0\leq i,j\leq M-1$. As illustrated by the algorithm 7, such projection is acceptable in practice. Indeed, let us assume that the updated quantities $\tilde{q}_u$ and $\tilde{q}_v$ leave the convex set $\mathcal{Q}$. If σ is small enough, $\tilde{q}_u$ and $\tilde{q}_v$ will go in an outer band of the frontier of the convex set $\mathcal{Q}$, the size of the band being monitored by the time step. Hence the norm of the residual is controlled with σ, this ensures that the quantities will be projected in an inner band of the frontier of the convex set $\mathcal{Q}$, the size of the band being also controlled with σ.

With this new convexification of the data term, the equivalence with the upper level set formulation does no longer hold, and the layer cake formula can no longer be used either. This is the reason why the authors of [27] proposed to build an admissible function of the original problem by keeping for each pixel x, the couple of labels (u_i, v_j) that maximize $w_u^*(x,u_i) + w_v^*(x,v_i)$. It leads in practice to noisy estimations. Moreover, as in the previous non convex approach, there is no way to show that the so-obtained estimation is a solution of the original non-linear problem. We will even see in the application section that it does not produce better estimations, in terms of energy, than the non convex approach.

Algorithm 7 Minimizing the 2D convex energy (4.9)

Initialize $w_u^0 = \bar{w}_u^0 = \frac{1}{M}$, $w_v^0 = \bar{w}_v^0 = \frac{1}{M}$,$\mathbf{z}_u^0 = \mathbf{z}_v^0 = q_u^0 = q_v^0 = 0$, chose $\theta \in [0,1]$ and $\sigma, \tau > 0$ such that $\sigma\tau < \frac{1}{8M^2}$

while $||w_u^k - w_u^{k-1}|| + ||w_v^k - w_v^{k-1}|| > \epsilon$ **do**

$\mathbf{z}_u^{k+1}(.,u_i) = P_{\mathcal{B}}\left(\mathbf{z}_u^k(.,u_i) + \sigma D_x\left(\sum_{l\geq i} \bar{w}_u^k(.,u_l)\right)\right), \qquad \forall u_i \in \Gamma^u$

$\mathbf{z}_v^{k+1}(.,v_j) = P_{\mathcal{B}}\left(\mathbf{z}_v^k(.,v_j) + \sigma D_x\left(\sum_{l\geq j} \bar{w}_v^k(.,v_l)\right)\right), \qquad \forall v_j \in \Gamma^v$

$\tilde{q}_u(.,u_i) = q_u^k(.,u_i) + \sigma \bar{w}_u^k(.,u_i)$

$\tilde{q}_v(.,v_j) = q_v^k(.,v_j) + \sigma \bar{w}_v^k(.,v_j)$

$[q_u^{k+1}, q_v^{k+1}] = P_{\mathcal{Q}}([\tilde{q}_u, \tilde{q}_v])$

$\tilde{w}_u(.,u_i) = w_u^k(.,u_i) - \tau\left(q_u^{k+1}(.,u_i) + \sum_{l\leq i} D_x^* \mathbf{z}_u^{k+1}(.,u_l)\right), \qquad \forall u_i \in \Gamma^u$

$w_u^{k+1} = P_{\mathcal{D}}\left(\tilde{w}_u\right),$

$\bar{w}_u^{k+1} = w_u^{k+1} + \theta(w_u^{k+1} - \bar{w}_u^k)$

$\tilde{w}_v(.,v_j) = w_v^k(.,v_j) - \tau\left(q_v^{k+1}(.,v_j) + \sum_{l\leq j} D_x^* \mathbf{z}_v^{k+1}(.,v_l)\right), \qquad \forall v_j \in \Gamma^v$

$w_v^{k+1} = P_{\mathcal{D}}\left(\tilde{w}_v\right),$

$\bar{w}_v^{k+1} = w_v^{k+1} + \theta(w_v^{k+1} - \bar{w}_v^k)$

end while

Finally note that this process involves relations between all the pairs $(q_u(x,u_i), q_v(x,v_j))$, so that it will necessarily lead to stock additional variables of size $|\Omega|M^2$.

4.2. General convexification. We now look at another convexification that increases the primal dimension but allows gathering all the unknowns in a single auxiliary variable.

4.2.1. Convexification with upper level sets. As in [8], we can follow the strategy of section 3.1 and consider the function $\phi(x,u_i,v_j) = H(u(x)-u_i)H(v(x)-v_j)$ to convexify the problem (4.1). Note that since $H(u(x)-u_0) = H(v(x)-v_0) = 1$ we have $\phi(x,u_0,v_j) = H(v(x)-v_j)$ and $\phi(x,u_i,v_0) = H(u(x)-u_i)$. Observing that:

$$\begin{aligned}
&\int_\Omega \rho(x,u(x),v(x))dx \\
&= \int_\Omega \sum_{i,j=0}^{M-2} \rho(x,u_i,v_j)(H(u(x)-u_i) - H(u(x)-u_{i+1}))(H(v(x)-v_j) - H(v(x)-v_{j+1}))\,dx \\
&= \sum_{i,j=0}^{M-1} \int_\Omega \rho(x,u_i,v_j)(\phi(x,u_i,v_j) - \phi(x,u_i,v_{j+1}) - \phi(x,u_{i+1},v_j) + \phi(x,u_{i+1},v_{j+1}))
\end{aligned} \tag{4.10}$$

$$\begin{aligned}\int_\Omega |Du(x)| =& \sum_{i=1}^{M-1} \int_\Omega (u_i - u_{i-1}) |D_x H(u(x) - u_i)| dx \\ =& \Delta_u \sum_{i=1}^{M-1} \int_\Omega |D_x \phi(x, u_i, v_0)| dx \qquad (4.11)\\ \int_\Omega |Dv(x)| =& \Delta_v \sum_{i=1}^{M-1} \int_\Omega |D_x \phi(x, u_0, v_i)| dx \qquad (4.12)\end{aligned}$$

we can then consider the functional $J(\phi)$ defined as the sum of the three terms (4.10), (4.11) and (4.12) and look at the convex problem

$$\min_{\phi \in \bar{\mathcal{A}}_2} J(\phi), \tag{4.13}$$

defined on the relaxed convex set of admissible functions:

$$\begin{aligned}\bar{\mathcal{A}}_2 = \{\phi : (x,s,t) \in BV(\Sigma, [0,1]),\ & \phi(x, u_0, v_0) = 1, \\ & \phi(x, u_i, v_j) - \phi(x, u_i, v_{j+1}) - \phi(x, u_{i+1}, v_j) + \phi(x, u_{i+1}, v_{j+1}) \geq 0 \\ & \phi(x, u_i, u_j) \geq \phi(x, u_{i+1}, v_j),\ \phi(x, u_i, u_j) \geq \phi(x, u_i, v_{j+1})\},\end{aligned}$$

where $\Sigma = \Omega \times \Gamma^u \times \Gamma^v$.

Hence, one can show that if the function ϕ^* is a binary minimizer of J, then the couple (u^*, v^*) defined as:

$$\begin{aligned}u^*(x) &= u_0 + \Delta_u \sum_{i=1}^{M-1} \phi(x, u_i, v_0) \\ v^*(x) &= v_0 + \Delta_v \sum_{i=1}^{M-1} \phi(x, u_0, v_i)\end{aligned} \tag{4.14}$$

is a global minimizer of the functional (4.1). However, if ϕ^* is not binary, we can not use relations (4.14) to build a solution of the original non convex problem. This is due to the fact that in the $2D$ case, the characteristic functions of the level sets of ϕ may not belong to the set of admissible functions $\mathcal{A}_2$, defined as:

$$\begin{aligned}\mathcal{A}_2 = \{\phi : (x,s,t) \in BV(\Sigma, [0,1]),\ & \phi(x, u_0, v_0) = 1, \\ & \phi(x, u_i, v_j) - \phi(x, u_i, v_{j+1}) - \phi(x, u_{i+1}, v_j) + \phi(x, u_{i+1}, v_{j+1}) \in \{0; 1\} \\ & \phi(x, u_i, u_j) \geq \phi(x, u_{i+1}, v_j),\ \phi(x, u_i, u_j) \geq \phi(x, u_i, v_{j+1})\}.\end{aligned}$$

This main issue will be discussed in section 5. As the projection on the derivative constraints included in the convex set $\mathcal{A}_2$ seems here unrealistic due to the complexity of the iterative Dijkstra algorithm that should be done pointwise, for each $x \in \Omega$, we now detail the equivalent probabilistic formulation that involves exact projections.

4.3. The $2D$ probabilistic point of view. A probabilistic formulation of the convexification for the $2D$ problem is now proposed. As in section 3.2, we introduce

the variable $w(x, u_i, v_j)$ measuring the probability of assigning the label pair $(u_i, v_j) \in \Gamma^u \times \Gamma^v$ to the pixel $x \in \Omega$. The data term now reads:

$$\min_{u\in\Gamma^u, v\in\Gamma^v} \int_\Omega \rho(x, u(x), v(x))dx = \min_{w\in\mathcal{D}_2} \int_\Omega \sum_{i=0}^{M-1}\sum_{j=0}^{M-1} \rho(x, u_i, v_j)w(x, u_i, v_j)dx,$$

where $\Sigma = \Omega \times \Gamma^u \times \Gamma^v$. The previous relation is valid for binary values of w with a single one that is 1 for each $x \in \Omega$. As before, since such class of functions is not convex, the set of admissible functions is relaxed as

$$\mathcal{D}_2 = \left\{ w : \Sigma \mapsto [0, 1], \text{ s.t. } \sum_{i=0}^{M-1}\sum_{j=0}^{M-1} w(x, u_i, v_j) = 1, \forall x \in \Omega \right\}. \tag{4.15}$$

Again, the Total Variation of u and v can be rewritten in terms of w as:

$$\int_\Omega |Du| = \Delta_u \int_\Omega \sum_{i=1}^{M-1} \left| D_x \sum_{j=1}^{M-1}\sum_{k\geq i} w(x, u_k, v_j) \right| dx$$
$$\int_\Omega |Dv| = \Delta_v \int_\Omega \sum_{j=1}^{M-1} \left| D_x \sum_{i=1}^{M-1}\sum_{k\geq j} w(x, u_i, v_k) \right| dx$$

The functional to minimize is then:

$$\begin{aligned} J_w(w) = &\int_\Omega \sum_{i=1}^{M-1}\sum_{j=1}^{M-1} \rho(x, u_i, v_j)w(x, u_i, v_j)dx + \Delta_u \int_\Omega \sum_{i=1}^{M-1} \left| D_x \sum_{j=1}^{M-1}\sum_{k\geq i} w(x, u_k, v_j) \right| dx \\ &+ \Delta_v \int_\Omega \sum_{i=j}^{M-1} \left| D_x \sum_{i=1}^{M-1}\sum_{k\geq j} w(x, u_i, v_k) \right| dx. \end{aligned} \tag{4.16}$$

The problem of minimizing (4.16) w.r.t $w \in \mathcal{D}_2$ is convex and a global minimum can be found with the previously introduced dual optimization methods. The process is summed up in Algorithm 8 and its preconditionned version in the Algorithm 9. The projection on $\mathcal{D}_2$ can also be done point-wise by projecting, for each pixel x the vector of coordinates $w(x, ., .)$ onto a simplex of dimension M^2, which make the primal projection exact, contrary to the upper level set formulation.

Equivalence between the relaxed problems. Probability and upper level sets formulations are equivalent, as in $1D$. Indeed, by taking $\phi(x, s, t) = H(u(x) - s)H(v(x) - t)$ and consider the problem $\min_{\phi\in\mathcal{A}_2} J(\phi)$. we find the same kind of relation than in section 3.2:

PROPOSITION 4.1. *There exists a bijection f between the convex sets $\mathcal{A}_2$ and $\mathcal{D}_2$, with $f(\phi)(x, u_i, v_j) = \phi(x, u_i, v_j) - \phi(x, u_i, v_{j+1}) - \phi(x, u_{i+1}, v_j) + \phi(x, u_{i+1}, v_{j+1})$ and $f^{-1}(w)(x, u_i, v_j) = \sum_{k\geq i}\sum_{l\geq j} w(x, u_k, v_l)$ and we have $J(\phi) = J_w(f(\phi))$.*

An example of such relation between local values of $w(x, ., .)$ and $\phi(x, ., .)$ is given in Figure 4.1. Note that the upper level set approach for $2D$ problems have also been

Algorithm 8 Minimizing the 2D convex energy (4.16)

Initialize $w^0 = \bar{w}^0 = \frac{1}{M^2}$,$\mathbf{z}_u^0 = \mathbf{z}_v^0 = 0$, chose $\theta \in [0,1]$ and $\sigma, \tau > 0$ such that $\sigma\tau < \frac{1}{16M^3}$

while $||w^k - w^{k-1}|| > \epsilon$ **do**

$\mathbf{z}_u^{k+1}(.,u_i) = P_{\mathcal{B}}\left(\mathbf{z}_u^k(.,u_i) + \sigma D_x\left(\sum_{l=0}^{M-1}\sum_{j\geq i}\bar{w}^k(.,u_j,v_l)\right)\right), \qquad \forall u_i \in \Gamma^u$

$\mathbf{z}_v^{k+1}(.,v_j) = P_{\mathcal{B}}\left(\mathbf{z}_v^k(.,v_j) + \sigma D_x\left(\sum_{l=0}^{M-1}\sum_{j\geq i}\bar{w}^k(.,u_l,v_j)\right)\right), \qquad \forall v_j \in \Gamma^v$

$\tilde{w}(.,u_i,v_j) = w_u^k(.,u_i) - \tau\Big(\rho(.,u_i,v_j) + \sum_{l\leq i} D_x^*\mathbf{z}_u^{k+1}(.,u_l) + \sum_{l\leq j} D_x^*\mathbf{z}_v^{k+1}(.,v_l)\Big)$,
$\forall u_i, v_j \in \Gamma^u \times \Gamma^v$

$w^{k+1} = P_{\mathcal{D}}(\tilde{w})$,

$\bar{w}^{k+1} = w^{k+1} + \theta(w^{k+1} - \bar{w}^k)$

end while

Algorithm 9 Minimizing the 2D energy with the preconditioned algorithm (4.16)

Initialize $w^0 = \bar{w}^0 = \frac{1}{M}$, $\mathbf{z}^0 = 0$, take $\sigma_{u,i} = \frac{1}{2iM}, \sigma_{v,i} = \frac{1}{2iM}, \tau_{i,j} = \frac{1}{(4(M+1-i))(4(M+1-j))}$.

while $||w^k - w^{k-1}|| > \epsilon$ **do**

$w^{k+1} = P_{\mathcal{D}}\left(\left(w^k(.,u_i,v_j) - \tau_{i,j}\left(\rho(.,u_i,v_j) + \sum_{l\leq i} D_x^*\mathbf{z}_u^{k+1}(.,u_l) + \sum_{l\leq j} D_x^*\mathbf{z}_v^{k+1}(.,v_l)\right)\right)_{i,j}\right)$

$\mathbf{z}_u^{k+1}(.,u_i) = P_{\mathcal{B}}\left(\mathbf{z}_u^k(.,u_i) + \sigma_{u,i} D_x\left(\sum_{l=0}^{M-1}\sum_{j\geq i}\bar{w}^k(.,u_j,v_l)\right)\right), \qquad \forall u_i \in \Gamma^u$

$\mathbf{z}_v^{k+1}(.,v_j) = P_{\mathcal{B}}\left(\mathbf{z}_v^k(.,v_j) + \sigma_{v,j} D_x\left(\sum_{l=0}^{M-1}\sum_{j\geq i}\bar{w}^k(.,u_l,v_j)\right)\right), \qquad \forall v_j \in \Gamma^v$

end while

0	0	0	0	0	0
0	0	0	0	0	0
0	0	0	0	0.4	0
0	0	0.2	0.2	0	0
0	0	0	0	0	0
0.2	0	0	0	0	0

$w^*(x,.,.)$

$\Leftrightarrow$

0	0	0	0	0	0
0	0	0	0	0	0
0.4	0.4	0.4	0.4	0.4	0
0.8	0.8	0.8	0.6	0.4	0
0.8	0.8	0.8	0.6	0.4	0
1	0.8	0.8	0.6	0.4	0

$\phi^*(x,.,.)$

FIG. 4.1. *On the left: example of values $w^*(x,.,.)$. On the right: corresponding values $\phi^*(x,.,.)$.*

recently proposed in [17], where the constraints associated to $\mathcal{A}_2$ are treated with an aditional auxiliary variable instead of using a Dijkstra algorithm , as done in [6] for 1D problems.

The next proposition is a straightforward consequence of what has been discussed so far:

PROPOSITION 4.2. *If w^* is a global minimizer of the functional J_w defined in (4.16) w.r.t $w \in \mathcal{D}_2$, then $\phi^* = f^{-1}(w^*)$ is a global minimzer of problem (4.13).*

The method can easily be extended to $N - D$ by following the previous approach and defining the corresponding convex set $\mathcal{D}_N$. With respect to the non convex approach of section 4, we here gain convexity. On the other hand, the dimension of the state explodes, as $|\Omega|M^N > MN|\Omega|$ for practical problems where $M >> 1$.

Moreover, the question remains in dimensions $N > 1$ of getting back to a minimizer of the original problem. This is a tough question, as explained in [11], since there may be no connections between the two minimizers. Notice that this issue is not considered in [27], and that the solution proposed in [8] is not satisfactory as will be explained in the next section.

5. How to get back to the original problem ?. In the 1D case, we know how to get a solution of the original problem from the relaxed one. In 2D the approach with upper level sets does not always give a solution since upper level sets do not always lie in the domain of the original problem. We discuss this further and propose strategies to go back to the domain of the original problem. We compare the energies of the original problem obtained by these strategies with some others strategies used for the previous formulations.

5.1. Box functions : where it works. In any dimension N, the layer cake formula is valid for the energy J so that

$$J(\phi^*) = \int_0^1 J(H(\phi^* - \mu))d\mu,$$

In dimension $N = 1$, the characteristic function of the level sets of ϕ also belong of the set of acceptable solutions $\mathcal{A}_1$, which means, as we have already seen in Theorem 3.2, that for almost every threshold $\mu \in [0, 1]$, $H(\phi^* - \mu)$ is a global solution of the convex and non convex problems. In 2D the layer cake formula is still true if we extend the energy to $BV(\Omega \times \Gamma^u \times \Gamma^v, [0, 1])$ but $H(\phi^* - \mu)$ is not bound to be in $\mathcal{A}_2$ and we can not conclude in general.

Next, following [8], we define the box functions set B_f as the set of functions such that for almost every threshold μ, $H(\phi(x, u_i, v_j)-\mu) = H(u_i-u_{k_{x,\mu}})H(v_j-v_{l_{x,\mu}})$. This definition is motivated by the fact that it is then possible to get back by thresholding to the definition domain of the original problem by choosing $(u(x), v(x)) = (u_{k_{x,\mu}}, v_{l_{x,\mu}})$ and we find a global minimum of the original energy. This is illustrated in Figure 5.1.

0	0	0	0	0	0
0	0	0	0	0	0
0.4	0.4	0.4	0.4	0.4	0
0.8	0.8	0.8	0.6	0.4	0
0.8	0.8	0.8	0.6	0.4	0
1	0.8	0.8	0.6	0.4	0

$\phi^*(x, ., .)$

0	0	0	0	0	0
0	0	0	0	0	0
1	1	1	1	**1**	0
1	1	1	1	1	0
1	1	1	1	1	0
1	1	1	1	1	0

$\mu = 0.3$

0	0	0	0	0	0
0	0	0	0	0	0
0	0	0	0	0	0
1	1	1	**1**	0	0
1	1	1	1	0	0
1	1	1	1	0	0

$\mu = 0.5$

0	0	0	0	0	0
0	0	0	0	0	0
0	0	0	0	0	0
1	1	**1**	0	0	0
1	1	1	0	0	0
1	1	1	0	0	0

$\mu = 0.7$

FIG. 5.1. *When $\phi^*(x, ., .)$ is a box function (on the left), then any level set $\mathbf{1}_{\phi^*(x,.,.)>\mu}$ is also a box function (examples are given for thresholds $\mu \in \{0.3; 0.5; 0.7\}$).*

Unfortunately, for general problems, we may have that ϕ^* is not a box function, so that recovering (u, v) involves ambiguities. A sketch of such ambiguity is given in Figure 5.2. Moreover, as the box function set is not convex, it is difficult to impose such a constraint in practice. Nevertheless, we show in Figure 5.3 the percentage of pixels where we do not find a box function after thresholding in an optical flow estimation. This shows that for real applications, where few global minima of the non convex energy are expected, we can expect recovering interesting solutions of the

original problem. Note that this result contradicts the analysis of [17], where the authors observe box functions everywhere on their results.

0	0	0	0	0	0
0	0	0	0	0	0
0.4	0.4	0.4	0.4	0	0
0.8	0.4	0.4	0.4	0	0
0.8	0.8	0.4	0.4	0	0
1	0.8	0.8	0.6	0	0

$\phi^*(x,.,.)$

0	0	0	0	0	0
0	0	0	0	0	0
1	1	1	**1**	0	0
1	1	1	1	0	0
1	1	1	1	0	0
1	1	1	1	0	0

$\mu = 0.3$

0	0	0	0	0	0
0	0	0	0	0	0
0	0	0	0	0	0
1	0	0	0	0	0
1	**1**	0	0	0	0
1	*1*	1	**1**	0	0

$\mu = 0.5$

0	0	0	0	0	0
0	0	0	0	0	0
0	0	0	0	0	0
1	0	0	0	0	0
1	**1**	0	0	0	0
1	*1*	**1**	0	0	0

$\mu = 0.7$

FIG. 5.2. *When $\phi^*(x,.,.)$ is not a box function (on the left), then its level sets $\mathbf{1}_{\phi^*(x,.,.)>\mu}$ have no reason to be box functions. Examples are given for thresholds $\mu \in \{0.3; 0.5; 0.7\}$. A box function is obtained with $\mu = 0.3$ but stairs functions are obtained with the other thresholds.*

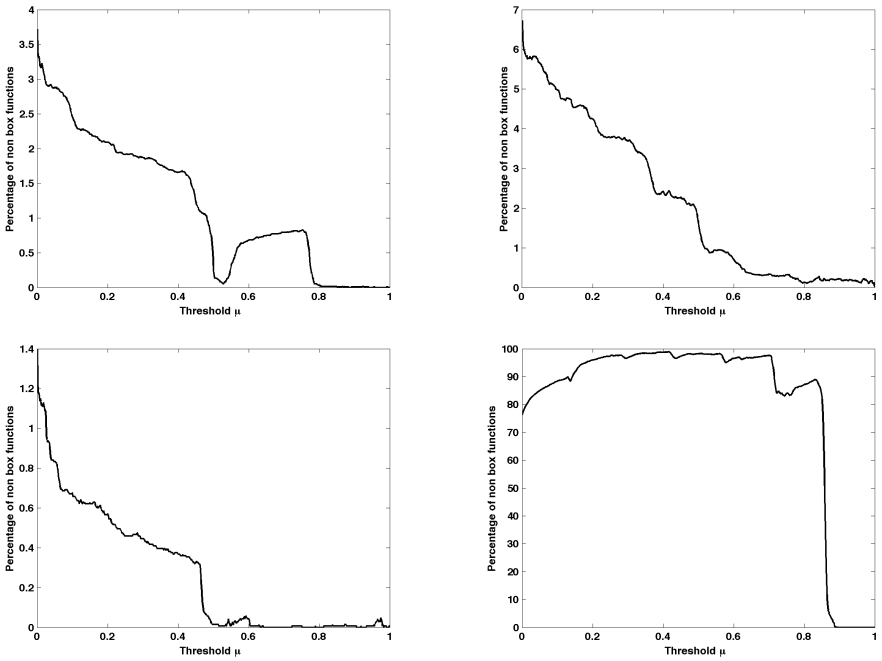

FIG. 5.3. *For any threshold $\mu \in]0,1[$, we plot the percentage of pixels where the function $H(\phi^* - \mu)$ is not a box function. These estimations have been done on 4 different data configurations, the last one being with random data, whereas the other correspond to realistic, where few global minima are expected.*

5.2. Stair functions. As we have seen, we can conclude in the case of box functions, but this case is not general enough for our purpose. Let us explain what happens in dimension 2, if we threshold $\phi_\mu = \phi^* \geq \mu$, then $\phi_\mu(x,s,t) \in \{0;1\}$, but $\phi_\mu(x,u_i,v_j) - \phi_\mu(x,u_i,v_{j+1}) - \phi_\mu(x,u_{i+1},v_j) + \phi_\mu(x,u_{i+1},v_{j+1}) \in \{-1;0;1\}$. With respect to $w_\mu = \partial_{st}\phi_\mu$, we will have $\sum_s \sum_t w_\mu(x,s,t) = 1$, but $w_\mu(x,s,t) \in \{-1;0;1\}$, which is not acceptable for a distribution.

Let us now assume that at a point x, $H(\phi^* - \mu)$ is not a box function, then $H(\phi^* - \mu)$ is necessarily a binary "stair function" defined in the set S_f:

$$S_f = \{\phi(s,t) : \phi(x,y) \geq \phi(s,t)\, \forall x < s,\, y < t)\}.$$

A sketch of binary stair functions is given in Figure 5.2. The trouble is that stair functions are not necessary box functions, so that the characteristic function of the level sets of ϕ^* do not necessary belong to the set of acceptable solutions $\mathcal{A}_2$.

This explains the reasoning of [8]. The authors advocate the threshold $\mu = 1$ that always lead to a binary box function. The trouble is that such a thresholding is not the best choice as we will see. Another solution to necessarily obtain a box function is to select one (if not unique) of the highest values of $w^*(x,.,.)$ for each $x \in \Omega$, but we will see that that such strategy is not optimal in practice.

5.3. How to choose a box function to approximate a solution of the original problem. In view of the discussion above, a solution to estimate u and v is to consider different thresholdings of ϕ^* that leads to box functions. Let us consider the box function $\phi^b_{\mu,\nu} = H(\phi^*(x,s,v_0) - \mu)H(\phi^*(x,u_0,t) - \nu)$

Regularization term case. We have that :

$$\begin{aligned}
&\int_\Omega \sum_{i=1}^{M-1} (u_i - u_{i-1}) |D_x \phi^b_{\mu,\nu}(x,u_i,v_0)| \\
&= \int_\Omega \sum_{i=1}^{M-1} (u_i - u_{i-1}) |D_x H(\phi^*(x,u_i,v_0) - \mu) H(\phi^*(x,u_0,v_0) - \nu)| \\
&= \int_\Omega \sum_{i=1}^{M-1} (u_i - u_{i-1}) |D_x H(\phi^*(x,u_i,v_0) - \mu)| \\
&\int_\Omega \sum_{i=1}^{M-1} (v_i - v_{i-1}) |D_x \phi^b_{\mu,\nu}(x,u_0,v_i)| \\
&= \int_\Omega \sum_{i=1}^{M-1} (v_i - v_{i-1}) |D_x H(\phi^*(x,u_0,v_i) - \nu)|.
\end{aligned}$$

Denoting as J_{TV}, the total variation part of the energy J, thanks to the coarea formula we therefore see that:

$$\begin{aligned}
&\int_{\mu=0}^1 \int_{\nu=0}^1 J_{TV}(\phi^b_{\mu,\nu}) \\
&= \int_{\mu=0}^1 \int_{\nu=0}^1 \left(\int_\Omega \sum_{i=1}^{M-1} (u_i - u_{i-1}) |D_x \phi^b_{\mu,\nu}(x,u_i,v_0)| + \int_\Omega \sum_{i=1}^{M-1} (v_i - v_{i-1}) |D_x \phi^b_{\mu,\nu}(x,u_0,v_i)| \right) \\
&= \int_{\mu=0}^1 \int_{\nu=0}^1 \left(\int_\Omega \sum_{i=1}^{M-1} (u_i - u_{i-1}) |D_x H(\phi^*(x,u_i,v_0) - \mu)| \right. \\
&\quad \left. + \int_\Omega \sum_{i=1}^{M-1} (v_i - v_{i-1}) |D_x H(\phi^*(x,u_0,v_i) - \nu)| \right) \\
&= \int_\Omega \sum_{i=1}^{M-1} (u_i - u_{i-1}) |D_x \phi^*(x,u_i,v_0)| + \int_\Omega \sum_{i=1}^{M-1} (v_i - v_{i-1}) |D_x \phi^*(x,u_0,v_i)| \\
&= J_{TV}(\phi^*)
\end{aligned}$$

Data term case. For the data term J_{Data}, we would want $\int_{\mu=0}^{1}\int_{\nu=0}^{1}\phi^b_{\mu,\nu} = \phi^*$, but

$$\begin{aligned}\int_{\mu=0}^{1}\int_{\nu=0}^{1}\phi^b_{\mu,\nu} &= \int_{\mu=0}^{1}\int_{\nu=0}^{1} H(\phi^*(x,s,v_0)-\mu)H(\phi^*(x,u_0,t)-\nu)\\ &= \phi^*(x,s,v_0)\phi^*(x,u_0,t).\end{aligned} \tag{5.1}$$

So if $\phi^*(x,s,v_0)\phi^*(x,u_0,t) = \phi^*(x,s,t)$ or in terms of w if u and v are independent, then we can find a global solution of the original problem for almost any threshold (μ,ν).

If this is not the case, coming back to the upper level sets $\phi^*_\mu = H(\phi^*-\mu)$, one knows that the points (s,t) such that $\phi^*_\mu(x,u_i,v_j) - \phi^*_\mu(x,u_i,v_{j+1}) - \phi^*_\mu(x,u_{i+1},v_j) + \phi^*_\mu(x,u_{i+1},v_{j+1}) = 1$ should correspond to high probabilities $w(x,s,t)$, one could then observe that choosing one of these couples to build a box function should be better for the data term of the energy. We denote by (s^i,t^i) these $n_x \geq 1$ points. For each point x and each extremal point (s^i,t^i), we can therefore define a box function $\phi^b_i(x,s,t) = H(s^i-s)H(t^i-t)$. The two box functions associated to the particular extremal points (s^1,t^1) and (s^{n_x},t^{n_x}) are then represented as ϕ^b_1 and ϕ^b_n.

With these notations, the box function $\phi^b_{\mu,\mu}$ is the smallest one to include the binary stair function $H(\phi^*-\mu)$. The coordinates of such box function are represented with the couple of point (s^*,t^*). An illustration of this is given in Figure 5.4 to explicit all these cases.

0	0	0	0	0	0	0
0	0	0	0	0	0	0
$\underset{\mathbf{1}}{(s^4,t^4)}$	0	0	0	$\underset{\mathbf{0}}{(s^*,t^*)}$	0	0
1	$\underset{\mathbf{1}}{(s^3,t^3)}$	0	0	0	0	0
1	1	1	$\underset{\mathbf{1}}{(s^2,t^2)}$	0	0	0
1	1	1	1	$\underset{\mathbf{1}}{(s^1,t^1)}$	0	0
1	1	1	1	1	0	0

FIG. 5.4. *The thresholded solution $H(\phi^*-\mu)$ is given, and the different possible natural binary box functions are shown (defined with the pairs of labels (s,t)). We here have $n_x = 4$.*

As a consequence, setting $J_{TV} = J_u + J_v$, we could expect that:
- $J_{TV}(\phi^b_{\mu,\mu}) = J_{TV}(\phi^*_\mu) \approx J_{TV}(\phi^*)$ and there is no prior on $J_{Data}(\phi^b_{\mu,\mu})$
- $J_u(\phi^b_1) = J_u(\phi^*_\mu) \approx J_u(\phi^*)$, $J_{Data}(\phi^b_1) \approx J_{Data}(\phi^*)$ and there is no prior on $J_u(\phi^b_1)$
- $J_v(\phi^b_n) = J_v(\phi^*_\mu) \approx J_v(\phi^*)$, $J_{Data}(\phi^b_N) \approx J_{Data}(\phi^*)$ and there is no prior on $J_v(\phi^b_N)$

The energies for the three previously mentioned particular box functions derived from $H(\phi^*-\mu)$ are given in Table 5.5. These results demonstrate numerically what has been detailed before, apart from the fact that the data term is increasing for large $\mu > 0.5$. This is due to the fact that in the present experiment, the estimated $w(x,.,.)$ appeared to be either unimodal or bimodal for almost any $x \in \Omega$.

It can be noticed that the first thresholding choice (where the regularization term is controlled by selecting a box function with the pairs (s^*,t^*)) seems to lead to good results in all the cases. We will therefore consider such a thresholding approach in

the following. The best threshold is around $\mu = 0.5$ and we will consider this value from now on. This experiment also shows that the strategy of [8] is not optimal, as the threshold $\mu = 1$ leads to a worse energy.

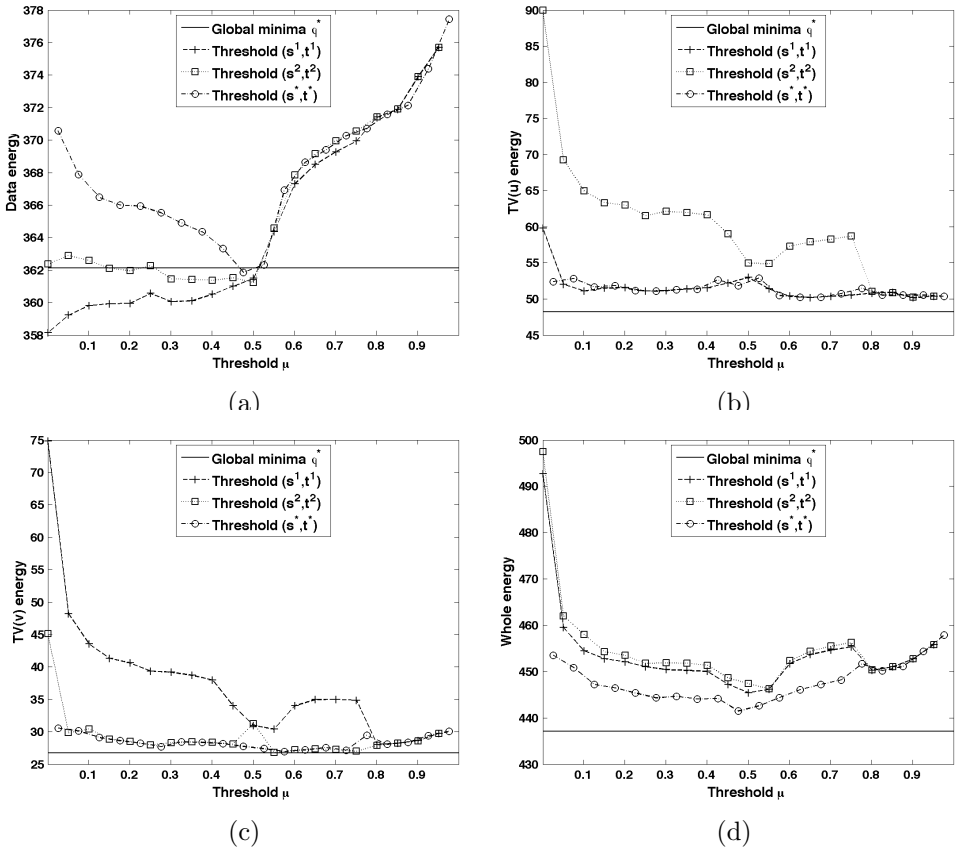

FIG. 5.5. *The energy of the computed global minima ϕ^* is compared to the eneries of the different thresholding approaches to obtain box functions. (a) Data term. (b) Tv(u). (c) TV(v). (d) Complete energies ((a)+(b)+(c)).*

Remark. Recalling the equivalence between w and ϕ described Figure 4.1, it is interesting to see that box functions will be found anytime as long as we can define, for every $x \in \Omega$ a non decreasing path (s^k, t^k) with $s^{k+1} \geq s^k$ and $t^{k+1} \geq t^k$ that crosses all the non null weights $w(x, s, t)$. Naturally, if we can define for every $x \in \Omega$ a path (s^k, t^k) with $s^{k+1} \leq s^k$ and $t^{k+1} \geq t^k$, then we would have box functions by taking the upper level sets of u and the lower level sets of v. Having such the same configuration of weights for all pixels has nevertheless no reason to occur in general.

5.4. Quality Indicator. The estimated global minima w^* of the relaxed energy can be used to define an empirical quality criterion. We know that if $w^*(x, ., .)$ is unimodal for any $x \in \Omega$, then w^* will give a feasible optimal solution of the original non convex problem. As a consequence, we can measure how $w^*(x, ., .)$ is far from an unimodal distribution. This will give an indication of the possibilities of having non-box functions when thresholding the global minima. To that end, we first define the mean estimation given by: $\bar{u}(x) = \sum_{i=1}^{M} \sum_{j=1}^{M} u_i w(x, u_i, v_j)$, $\bar{v}(x) = \sum_{i=1}^{M} \sum_{j=1}^{M} v_j w(x, u_i, v_j)$. Then, the dispersion of the distribution is measured

with: $d_w(x) = \sum_{i=1}^{M}\sum_{j=1}^{M} w(x,u_i,v_j)\left((u_i-\bar{u}(x))^2+(v_j-\bar{v}(x))^2\right)$, and normalized (using that the maximum value of $d_w(x)$ is $\frac{M^2}{2}$) to obtain the following Quality Indicator:

$$QI(w) = 1. - \left(\int_{x\in\Omega} \frac{2d_w(x)}{|\Omega|M^2}\right)^{-\frac{1}{2}},$$

that will tend to 1 (resp. 0) as soon as $w(x,.,.)$ is unimodal (resp. uniform). As a consequence, we can see that the energy of the original problem recovered from w^* will be very close to global minima of the relaxed energy if $QI(w^*) \to 0$. The computed value then indicates the level of possibility of recovering a bad solution of the original problem.

5.5. Comparison with the other approaches. With respect to the non convex approach [23] (which is a lot faster), the solutions obtained with our convex approach (taken with $\phi^b_{\mu,\mu}$ and $\mu = 0.5$) always have smaller energies. We also reach the same global energy minima than the ones obtained with the convexification of the data term [27]. This is illustrated in Table 5.1, where the energies estimated by the convex and non convex approaches are presented for a real optical flow experiment. As suggested in [27], we also show the energies obtained by keeping the most probable value for every $x \in \Omega$, that leads to bad estimations for the convex approaches. We also computed the energy associated with the weighted mean value, but do not present them as it gives worse results in practice. As expected, the solutions obtained with the convex approaches are independent from the initialization. Note that when increasing the number of labels, the non convex approach is also more frequently stuck in poor local minima.

	Relaxed energy: minima estimation	Original energy: best threshold	Original energy: highest probability
Uniform initialization			
Non convex [23]	441.73 (QI 0.984)	444.55 (+0.64%)	445.02 (+0.75%)
Data convexified [27]	436.56 (QIk 0.66)	467.01 (+6.98%)	541.74 (+24.09%)
Proposed convex	437.11 (QI 0.969)	441.40 (+0.98%)	454.76 (+4.04)%)
Best label initialization			
Non convex [23]	479.56 (QI 0.98)	481.29 (+0.36%)	481.77 (+0.46%)
Data convexified [27]	436.85 (QI 0.66)	466.01 (+6.67%)	539.35 (+23.46%)
Proposed convex	437.15 (QI 0.969)	441.43 (+0.98%)	456.47 (+4.42%)
Random initialization			
Non convex [23]	538.40 (QI 0.972)	541.67(+0.61%)	542.97 (+0.85%)
Data convexified [27]	437.12 (QI 0.66)	466.74 (+6.78%)	539.13 (+23.34%)
Proposed convex	437.12 (QI 0.969)	441.44 (+0.99%)	455.66 (+4.24%)

TABLE 5.1

Comparison for a real example. The energies of the minima of the relaxed problems obtained with the different methods and different initializations (uniform, best label without regularization and random) are given in the first column. The original energy is then computed for the solution built by thresholding the corresponding upper level set function (second column) or by keeping the label with the highest probability (last column). The convex approaches lead to the same global minima for any initialization. The non convex approach allows recovering solutions of the original problem whose energies are close to the one of the local solution estimated for the relaxed problem.

We show in Figure 5.6 that the non convex method and the proposed convex method gives reasonable estimations (in terms of energy) for any threshold, whereas

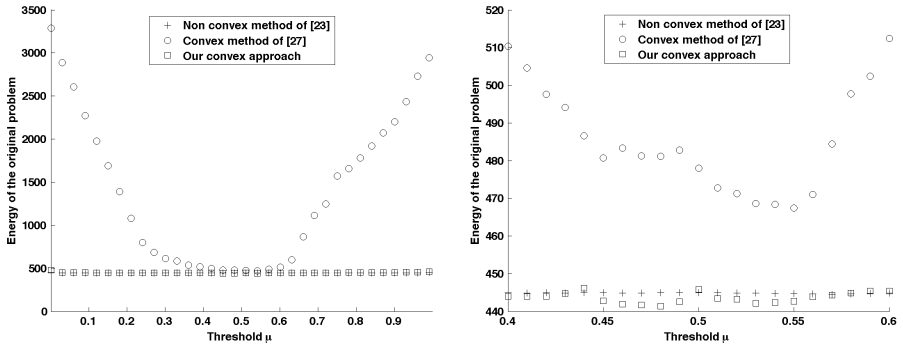

(a) (b)

FIG. 5.6. *Comparison of thresholded solutions. (a) The convex approach of [27] gives very bad estimations for threshold far from* $\mu = 0.5$. *(b) A zoom of the plot is given for threshold in the interval* $[0.4; 0.6]$.

the convex method of [27] is more sensible to thresholding values. This is also illustrated by the Quality Indicator that is always far from 1 with the method of [27]. As expected, the Quality Indicator here shows that the thresholded solution will have energies close to the computed minima with the non convex approach and the proposed convex method. The corresponding optical flow estimations are given in the Figure 6.5 of next section. Note that in this example realized on a realistic data configuration, we expect the modeling to be well suited, so that the original non convex problem should have few global minima. This explains why the recovered solutions give satisfying energies.

These examples have been obtained by considering $M_u = 8$ and $M_v = 7$ labels. One can observe that the required memory needed by each approach is:

- Non convex : $3(M_u + M_v)|\Omega|$, as ρ_u, w_u, and $\mathbf{z}_u$ are of size $M_u|\Omega|$, while ρ_v, w_v and $\mathbf{z}_v$ are of size $M_v|\Omega|$
- Convex [27]: $(3M_u+3M_v+M_uM_v)|\Omega|$, as w_u, q_u and $\mathbf{z}_u$ are of size $M_u|\Omega|$ and ρ of size $M_uM_v|\Omega|$ (the original method also requires an aditionnal lagrange multiplier of size $M_uM_v|\Omega|$).
- Our approach: $(M_u + M_v + 2M_uM_v)|\Omega|$,as $\mathbf{z}_u$ is of size $M_u|\Omega|$ and ρ and w of size $M_uM_v|\Omega|$.

This shows that the proposed approach doe not take more memory than the original approach of [27], while it gives more accurate results. Note that in all cases, the required memory could be reduced by computing the cost variables ρ when needed, but this would drastically increase the computational cost.

We finally show in Table 5.2 the same kind of results for random data ρ. We also observe that the convex approaches allow to estimate a better minima of the relaxed energy. However, as the data are totally random, the TV denoising is here not a good model. As a consequence, there are no reasons to recover unimodal probabilities. Hence, when thresholding the solutions given by the convex approaches, it here leads to very bad estimations for the original non convex problem, whereas the non convex approach still allows recovering acceptable solutions for the original problem. The Quality Indicator associated to the computed minima is here very informative for our approach, whereas it gives the same kind of values than for non random data for the method of [27]. This shows that, contrary to our convex approach, it seems impossible to have a prior information on the quality of the estimation computed with

the convex method of [27] that appears to be not favoring the estimation of unimodal distributions.

	Relaxed energy: minima estimation	Original energy: best threshold	Original energy: highest probability
Non convex [23]	6596 (QI 0.94)	6622.2 (+0.4%)	6622.9 (+0.4%)
Data convexified [27]	6207 (QI 0.6)	6829 (+10%)	16352 (+163%)
Proposed convex	6208 (QI 0.62)	6714 (+8.1%)	12385 (+99.5%)

TABLE 5.2

The energies of the minima of the relaxed problems obtained with the different methods for random data ρ are given in the first column. The original energy is then computed for the solution built by thresholding the corresponding upper level set function (second column) or by keeping the label with the highest probability (last column).

We can therefore conclude that:
- The level sets of the solution ϕ^* obtained with the non convex approach have almost the same energy than ϕ^*, but it is not the case for the solution obtained with the convex method
- The proposed thresholding method associated to our convex method seem good enough for real applications (since the energy is not so far after thresholding to a box function)
- The non convex approach gives quite good local minima when a non random initialization is made. This validates experimentally the work of [23].

6. Applications. In this section, we present some numerical results obtained for multi-label problems involving up to $N = 3$ dimensions.

6.1. The $1D$ case.

6.1.1. Color based segmentation. Given one grayscale image I, we look at the segmentation problem

$$J_1(u) = \lambda \int_\Omega |Du(x)| + \int_\Omega |I(x) - u(x)| dx. \tag{6.1}$$

With u taking its values in $\Gamma^u = \{0 < 1/(M-1) \cdots < 1\}$. This corresponds to take $\rho(x, u(x)) = |I(x) - u(x)|$ and we apply Algorithm 5. This is a simple case as the data term ρ is here convex w.r.t u. The result obtained for $\lambda = 10$ and $M = 9$ are presented in Figure 6.1 and compared to the method of [25] (Algorithm 3). The obtained segmentations as well as the computational times are here equivalent, whereas our projection is exact.

I Our method [25]

FIG. 6.1. *Comparison of the results with [25] with the same parameters $M = 9$ and $\lambda = 4$. Both methods are equivalent.*

6.1.2. Disparity. Given two rectified images I_1 and I_2, (presented in Figure 6.2), we look at the disparity estimation problem

$$J_1(u) = \lambda \int_\Omega |Du(x)| + \int_\Omega |I_1(x) - I_2(x + u(x)|dx, \tag{6.2}$$

with u taking its values in $\Gamma^u = \{4 = u_0 < \cdots < u_{M-1} = 16\}$ and $\lambda = 7$. The data term is non convex as we have $\rho(x, u(x)) = |I_1(x) - I_2(x + u(x)|$. The result obtained with Algorithm 5 is presented in Figure 6.3 and compared with the method of [25] obtained with Algorithm 4, Figure 6.3 shows that both methods are equivalent.

I_1 I_2 u_{truth}

FIG. 6.2. *Stereo data and disparity ground truth.*

Our method [25]

FIG. 6.3. *Comparison of the method with [25] with the same parameters $M = 13$ and $\lambda = 7$. We recover exactlty the same dispartity maps.*

6.2. $2D$ **optical flow.** The optical flow between the images shown in 6.4 has been computed with various approaches: Non convex (Algorithm 6), Convex [27] (Algorithm 7) and proposed convex (Algorithm 9). The results are presented in Figure 6.5. It illustrates that the non convex approach leads to good estimations when initialized with uniforms probabilities.

I_1 I_2 $(u, v)_{truth}$

FIG. 6.4. *Images I_1 and I_2 of the RubberWhale sequence. The optical flow ground truth is presented, the color representing the direction of the flow, while the intensity is related to the norm of the vector.*

The convex approaches are more sensible to thresholding, namely the one of [27]. Note that the proposed approach allows to recover a thresholded solution with the lower energy, as illustrated in Table 5.1.

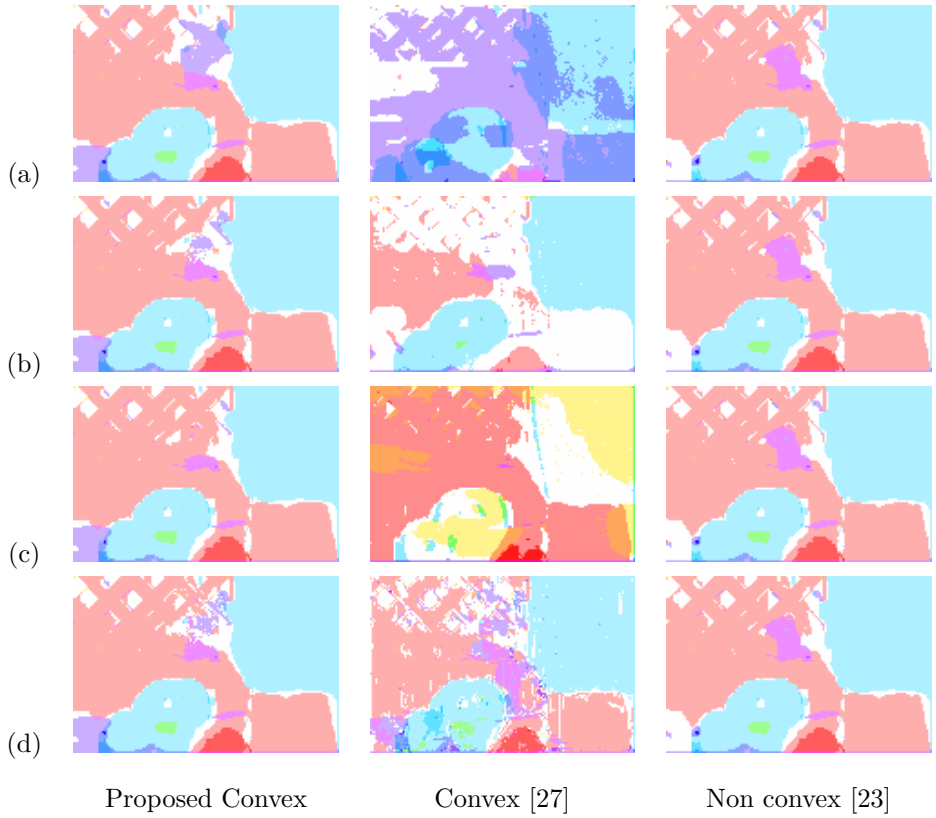

FIG. 6.5. *Comparison of the optical flow between I_1 and I_2 of Figure 6.4 estimated with the proposed convex, convex of [27] and non convex [23] approaches for different thresholds (a: $\mu = 0.4$, b: $\mu = 0.5$, c:$\mu = 0.6$) or highest probability (d). For this simple experiments realized on images of size 146×97 (a 25% rescale of the original size to let the methods converge in reasonable time), we set $\lambda = 0.04$ and only used 8×7 labels in order to visualize the difference between the methods. Note that these results correspond to the Table 5.5, so that the energy of the relaxed solution of [27] is the global minima, but the thresholded solutions are noisy. The proposed convex method allows recovering better solutions of the original problem. The non convex method is less sensible to thresholding.*

In Figure 6.6, we show the results corresponding to the three methods on the Hamburg taxi sequence. The images are of size 256×190 and we took $\lambda = 0.1$ and considered 9×9 labels. The different energies and computational details are given in Table 6.1.

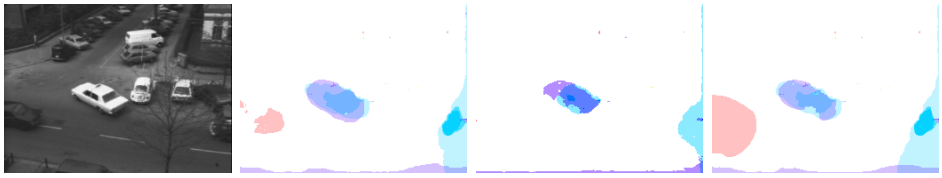

FIG. 6.6. *Results obtained after thresholding with $\mu = 0.5$, for the estimation of the optical flow between 2 frames of the Hamburg Taxi sequence. All three methods give good thresholded results as the regularization coefficient is here higher, which increases the convexity of the problem.*

The regularization parameter is here larger than in the previous experiments. This increases the convexity of the problem and all methods here give good thresholded solutions. In particular, the approach of [27] present a better behavior (as illustrated by the Quality indicator given in Table 6.1). Note that the code has been parallelized on GPU, but not fully optimized, so that better computational times could be expected, as the ones mentioned in [27] (1 minute for 256×256 images and 32×32 labels).

	Relaxed energy: minima estimation	Original energy: threshold $\mu = 0.5$	Computational time
Non convex [23]	1616 (QI 0.983)	1628 (+0.7%)	150s
Data convexified [27]	1613(QI 0.55)	1675 (+3.8%)	220s
Proposed convex	1614 (QI 0.93)	1631 (+1.1%)	250s

TABLE 6.1

First column: Relaxed energies obtained with the different methods for the estimation of the optical flow between two frames of the Hamburg taxi sequence. Second column: The original energy is computed for the solution built by thresholding the corresponding upper level set function. Last column: the computational time needed to reach the same level of residual between 2 *iterations.*

As the non convex approach leads to very accurate results while being faster to the convex ones, we show in Figure 6.7 the kind of estimations that can be obtained with an additional non convex narrow band approach [6] that allows speeding up the non convex process by only performing the calculations in the neighborhood of the current estimated labels. Such an approach then leads to interesting computational costs, while giving accurate estimations, as illustrated in Table 6.2.

FIG. 6.7. *Results obtained with the non convex approach on the Middlebury data Dimetrodon and Rubberwhale. The original images are shown in the first and second columns. The true optical flow in the third column is then compared to the estimated one in the forth.*

Images	RMSE	N_u	N_v	Time
Dimetrodon	0.22	51	51	20s
RubberWhale	0.36	31	31	5s

TABLE 6.2

Quantitative results of the non convex approach coupled with a narrow band method applied on the Middlebury optical flow benchmark datasets containing images of size 584×388. *The RMS Error between estimation and ground truth is given for the* 2 *studied examples.*

6.3. Experiments for $N = 3$. We now show some experiments involving higher dimensions. The following results have been obtained by extending the Algorithm 9 to dimensions 3.

6.3.1. Optical flow with occlusion mask. In order to enhance the optical flow modeling, one could also consider the simultaenous estimation of the occlusion mask. This comes to increase with one other dimension to model the occlusion mask. We then have as data term:

$$\rho(x, u(x), v(x), m(x)) = |I_1(x) - I_2(x + w(x))|(1 - m(x)) + \kappa m(x),$$

where $m(x) \in [0, 1]$ represent the occlusion map and $\kappa \geq 0$ is the occlusion cost. As occlusions form connex areas, the occlusion map can therefore be spatially regularized by minimizing:

$$\beta \int_\Omega |\nabla m|,$$

with $\beta > 0$. An example of estimation with $\kappa = 40/255$, $\beta = 0.005$, $\lambda = 0.04$ and comparisons with the proposed convex method (without occlusion mask) as well as the non convex method are given in Figure 6.8. This illustrates the ability of the method to deal with larger dimensions and simultaneously estimate information of different nature (flow and mask) in a convex way.

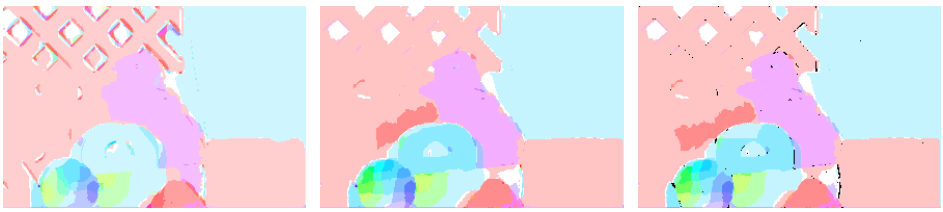

Non convex Convex Convex+occlusion

FIG. 6.8. *Solutions obtained on the image RubberWhale of size* 292×196 *(rescaled at* 50% *of its original size) with* 10×9 *labels. The occlusions are represented with black pixels.*

6.3.2. The Chan and Vese model. We finally consider the Chan and Vese model:

$$J(u, c_0, c_1) = \int_\Omega ||I - c_0||^2 u dx + \int_\Omega ||I - c_1||^2 (1 - u) dx + \lambda \int_\Omega |Du|$$

Following [8], we convexify the problem by considering the function $w(x, r, s, t) = \delta(u(x) = r)\delta(c_0 = s)\delta(c_1 = t)$ and follow the strategy of [8], which gives us a data cost:

$$\rho(x, r, s, t) = ||I - s||^2 r + ||I - t||^2 (1 - r).$$

With this formulation, we have to consider maps of constants $c_0(x)$ and $c_1(x)$ and add additional terms: $\kappa \int_\Omega |Dc_0|$ and $\kappa \int_\Omega |Dc_1|$ to the energy, with $\kappa \to \infty$, to ensure recovering constants. The problem is nevertheless ill-posed. Indeed, if (u, c_0, c_1) is a solution, so is $(1 - u, c_1, c_0)$, and also $(1/2, (c_1 + c_0)/2, (c_1 + c_0)/2)$, with convexity. A constraint like $c_0 < c_1$ should be added. It could be done by adding the penalization: $\epsilon(\int_\Omega ||c_0||^2 dx + \int_\Omega ||1 - c_1||^2 dx)$ or better by defining the domain of search as $s \leq t$, which correspond to only treat half of the possibilities.

We applied such a framework as illustrated in Figure 6.9 with a set of possible labels $[0; \frac{1}{4}; \frac{1}{2}; \frac{3}{4}; 1]$ which gives us the estimation $c_0 = \frac{1}{4}$ and $c_1 = \frac{3}{4}$. By injecting

FIG. 6.9. *Solution obtained with the full convex model* (u^*, c_0^*, c_1^*). *The image* u_2^* *denotes the solution obtained when fixing* $c_0 = \frac{1}{4}$ *and* $c_1 = \frac{3}{4}$. *We see that* $u^* = u_2^*$, *which means that the recovered solution* u^* *should be optimal.*

these estimated constants c_0 and c_1 in a classic TV segmentation model, where c_0 and c_1 are fixed [28], we even exactly recover the same segmentation map with the same energy. It shows that the thresholded solutions are optimal in practice.

REFERENCES

[1] L. AMBROSIO, N. N. FUSCO, AND D. PALLARA, *Functions of Bounded Variation and Free Discontinuity Problems*, Oxford Math. Monogr., The Claredon Press, Oxford University Press, 2000.

[2] G. AUBERT AND J-F. AUJOL, *Optimal partitions, regularized solutions, and application to image classification*, Applicable Analysis, 84 (2005), pp. 15–35.

[3] ———, *A variational approach to remove multiplicative noise*, SIAM Journal on Applied Mathematics, 68 (2008), pp. 925–946.

[4] G. AUBERT AND P. KORNPROBST, *Mathematical Problems in Image Processing*, vol. 147, Springer-Verlag, 2002.

[5] J-F. AUJOL, S. MASNOU, AND S. LADJAL, *Exemplar-based inpainting from a variational point of view*, SIAM Journal on Mathematical Analysis, 42 (2010), pp. 1246–1285.

[6] A. BAEZA, P. GARGALLO, V. CASELLES, AND N. PAPADAKIS, *A narrow band method for the convex formulation of discrete multi-label problems*, Multiscale Modeling & Simulation, 8 (2010), pp. 2048–2078.

[7] J.-M. BALL, *Convexity conditions and existence theorems in nonlinear elasticity*, Archive for Rational Mechanics and Analysis, 63 (1976), pp. 337–403.

[8] E. S. BROWN, . F. CHAN, AND X. BRESSON, *Completely convex formulation of the chan-vese image segmentation model*, Int. J. Comput. Vision, 98 (2012), pp. 103–121.

[9] A. CHAMBOLLE, *An algorithm for mean curvature motion*, Interfaces and Free Boundaries, 6 (2004), pp. 1–24.

[10] A. CHAMBOLLE, D. CREMERS, AND T. POCK, *A convex approach for computing minimal partitions*, Tech. Report 649, Technical Report CMAP, 2008.

[11] A. CHAMBOLLE, D CREMERS, AND T. POCK, *A convex approach to minimal partitions*, tech. report, Technical Report http://hal.archives-ouvertes.fr/hal-00630947, 2011.

[12] A. CHAMBOLLE AND T. POCK, *A first-order primal-dual algorithm for convex problems with applications to imaging*, Journal of Mathematical Imaging and Vision, 40 (2011), pp. 120–145.

[13] T. F. CHAN AND L. A. VESE, *Active contours without edges*, IEEE Transactions on Image Processing, 10 (2001), pp. 266–277.

[14] Y. CHEN AND X. YE, *Projection onto a simplex*, ArXiv e-prints, (2011).

[15] P.L. COMBETTES AND V. WAJS, *Signal recovery by proximal forward-backward splitting*, SIAM J. on Multi. Model. and Simu., 4 (2005).

[16] B. GOLDLUECKE AND D. CREMERS, *Convex relaxation for multilabel problems with product label spaces*, in European conference on Computer vision (ECCV'10), ECCV'10, 2010, pp. 225–238.

[17] T. GOLDSTEIN, X. BRESSON, AND S. OSHER, *Global minimization of markov random fields with applications to optical flow*, Inverse Problems and Imaging, 6 (2012), pp. 623–644.

[18] K. KOLEV, M. KLODT, T. BROX, AND D. CREMERS, *Continuous global optimization in multiview*

3d reconstruction, International Journal of Computer Vision, 84 (2009), pp. 80–96.
[19] P. Maurel, J-F. Aujol, and G. Peyré, *Locally parallel texture modeling*, SIAM Journal on Imaging Sciences, 4 (2011), pp. 413–447.
[20] J.J. Moreau, *Proximité et dualité dans un espace hilbertien*, Bulletin de la S.M.F, 93 (1965).
[21] D. Mumford and J. Shah, *Optimal approximation by piecewise smooth functions and associated variational problems*, Comm. Pure Appl. Math., 42 (1989), pp. 577–685.
[22] M. Nikolova, S. Esedoglu, and T. F. Chan, *Algorithms for finding global minimizers of image segmentation and denoising models*, SIAM Journal on Applied Mathematics, 66 (2006), pp. 1632–1648.
[23] N. Papadakis, A. Baeza, P. Gargallo, and V. Caselles, *Polyconvexification of the multi-label optical flow problem*, in Proc. IEEE Int. Conf. on Image Processing (ICIP'10), 2010.
[24] T. Pock and A. Chambolle, *Diagonal preconditioning for first order primal-dual algorithms in convex optimization*, in IEEE International Conference on Computer Vision (ICCV'11), 2011, pp. 1762 –1769.
[25] T.s Pock, T. Schoenemann, G. Graber, H. Bischof, and D. Cremers, *A convex formulation of continuous multi-label problems*, in Proceedings of the 10th European Conference on Computer Vision (ECCV'08): Part III, 2008, pp. 792–805.
[26] L. I. Rudin, S. Osher, and E. Fatemi, *Nonlinear total variation based noise removal algorithms*, Phys. D, 60 (1992), pp. 259–268.
[27] E. Strekalovskiy, B. Goldluecke, and D. Cremers, *Tight convex relaxations for vector-valued labeling problems*, in IEEE International Conference on Computer Vision (ICCV'11), 2011.
[28] R. Yildizoglu, J-F. Aujol, and N. Papadakis, *Active contours without level sets*, in Proc. IEEE Int. Conf. on Image Processing (ICIP'12), 2012.
[29] C. Zach, T. Pock, and H. Bischof, *A duality based approach for realtime tv-l1 optical flow*, in Proceedings of the 29th DAGM conference on Pattern recognition, 2007, pp. 214–223.